

**THE UNIVERSITY OF WESTERN ONTARIO  
DEPARTMENT OF CIVIL AND  
ENVIRONMENTAL ENGINEERING**

**Water Resources Research Report**

**ANEMI\_Yangtze**

**A regional integrated assessment model for  
the Yangtze Economic Belt in China**

**By:  
Haiyan Jiang,  
and  
Slobodan P. Simonovic**

**Report No: 111  
Date: February 2021**

**ISBN: (print) 978-0-7714-3155-5; (online) 978-0-7714-3156-2**



**ANEMI\_Yangtze**

**A regional integrated assessment model for the Yangtze Economic Belt in China**



**By**

**Haiyan Jiang**

**And**

**Slobodan P. Simonovic**

**Department of Civil and Environmental Engineering**

**Western University, Canada**

**Report No.111**

**February 2021**

## **Executive Summary**

Yangtze Economic Belt is one of the most dynamic regions in China in terms of population growth, economic progress, industrialization, and urbanization. It faces many resource constraints (food, energy) and environmental challenges (pollution, biodiversity loss) under rapid population growth and economic development. Interactions between human and natural systems are at the heart of the challenges facing the sustainable development of the Yangtze Economic Belt. Understanding these interactions poses challenges because human and natural systems evolve in response to a wide range of influences. Accounting for these complex dynamics requires a system tool that can represent the fundamental drivers of change and responses of the individual system as well as how different systems interact and co-evolve. By adopting the philosophy of system thinking and the methodology of system dynamics simulation, an integrated assessment model for the Yangtze Economic Belt, named ANEMI\_Yangtze, is developed based on the third version of the global integrated assessment model, ANEMI. Nine sectors of population, economy, land, food, energy, water, carbon, nutrients, and fish are currently included in ANEMI\_Yangtze.

This report identifies the opportunities and challenges facing the Yangtze Economic Belt and presents the development of the ANEMI\_Yangtze model structure. It also includes: (i) the identification of the cross-sectoral interactions and feedbacks involved in shaping Yangtze Economic Belt's system behaviour over time; (ii) the identification of the feedbacks within each sector that drive the state variables in the sector; and (iii) the explanation of the theoretical and mathematical basis for those feedbacks. ANEMI\_Yangtze was developed and calibrated sector by sector before coupling all of them together to complete the ANEMI\_Yangtze model. After the validation and robustness test, the ANEMI\_Yangtze model can be used to explore the potential impacts of climate change in the basin, to examine how changes in birth control policy affect population dynamics and the natural-environmental systems, to assess the effects of land-use change on food-water-carbon systems, to assess the impacts of shifting energy consumption patterns and water saving techniques, and to investigate how policies aimed at improving eco-environment situation affect the Yangtze Economic Belt system.

## Table of Contents

Executive Summary .....	i
Table of Contents .....	ii
<b>1. INTRODUCTION.....</b>	<b>1</b>
1.1 Water-Energy-Food Nexus .....	1
1.2 Integrated Assessment Model .....	1
1.3 Yangtze Economic Belt Opportunities and Challenges.....	3
<b>2. ANEMI_YANGTZE MODEL FRAMEWORK AND CROSS-SECTORAL FEEDBACKS .....</b>	<b>5</b>
2.1 Framework of ANEMI_Yangtze .....	5
2.2 Cross-sectoral Feedbacks in ANEMI_Yangtze .....	6
<b>3. ANEMI_YANGTZE MODEL STRUCTURE DESCRIPTION .....</b>	<b>10</b>
3.1 <i>Population Sector</i> .....	10
3.2 <i>Economy Sector</i> .....	12
3.3 <i>Land Sector</i> .....	14
3.4 <i>Food Sector</i> .....	16
3.5 <i>Energy Sector</i> .....	18
3.6 <i>Water Sector</i> .....	23
3.7 <i>Carbon Sector</i> .....	29
3.8 <i>Nutrients Sector</i> .....	34
3.9 <i>Fish Sector</i> .....	37
<b>4. MODEL VALIDATION AND SENSITIVITY ANALYSIS.....</b>	<b>40</b>
4.1 Model Validation.....	40
4.2 Sensitivity Analysis .....	41
<b>5. CLOSING REMARK.....</b>	<b>43</b>
<b>6. REFERENCES.....</b>	<b>44</b>
<b>Appendix A: STOCK AND FLOW DIAGRAM OF EACH SECTOR .....</b>	<b>49</b>

<b>Appendix B: MODEL AVAILABILITY .....</b>	<b>57</b>
<b>Appendix C: BASE RUN MODEL RESULTS .....</b>	<b>58</b>
<b>Appendix D: PREVIOUS REPORTS IN THE SERIES .....</b>	<b>63</b>

## List of Figures

Figure 1 Yangtze river basin (black dashed line) and the Yangtze Economic Belt .....	3
Figure 2 Framework of the ANEMI_Yangtze model .....	6
Figure 3 Interactions among the human-natural systems in the Yangtze Economic Belt .....	7
Figure 4 Causal feedback loops of the <i>Population Sector</i> .....	11
Figure 5 Causal feedback loops of the <i>Economy Sector</i> .....	13
Figure 6 Causal feedback loops of the <i>Food Sector</i> .....	17
Figure 7 Causal feedback loops of the <i>Energy Sector</i> .....	20
Figure 8 Causal feedback loops of the <i>Water Sector</i> .....	25
Figure 9 Causal feedback loops of the <i>Carbon Sector</i> .....	30
Figure 10 Causal feedback loops of the <i>Nutrients Sector</i> .....	35
Figure 11 Causal feedback loops of the <i>Fish Sector</i> .....	38
Figure 12 Comparison of simulated and historical system behaviours .....	40
Figure 13 Sensitivity of selected state variables .....	42
Figure 14 Total sensitivity of selected state variables .....	42
Figure A1 Stock and flow diagram of the <i>Population Sector</i> .....	49
Figure A2 Stock and flow diagram of the <i>Economy Sector</i> .....	50
Figure A3 Stock and flow diagram of the <i>Land Sector</i> .....	51
Figure A4 Stock and flow diagram of the <i>Food Sector</i> .....	52
Figure A5 Stock and flow diagram of the <i>Energy Sector</i> .....	53
Figure A6 Stock and flow diagram of the <i>Water Sector</i> .....	54
Figure A7 Stock and flow of the <i>Carbon Sector</i> .....	55
Figure A8 Stock and flow of the <i>Nutrients Sector</i> .....	56
Figure A9 Stock and flow of the <i>Fish Sector</i> .....	56
Figure A10 Socio-economic behaviours of the Yangtze Economic Belt .....	58
Figure A11 <i>Energy Sector</i> system behaviours of the Yangtze Economic Belt .....	58
Figure A12 System behaviours in the <i>Food Sector</i> of the Yangtze Economic Belt .....	59
Figure A13 System behaviours of water demand in the Yangtze Economic Belt .....	60
Figure A14 System behaviours of water stress in the Yangtze Economic Belt .....	61
Figure A15 Eco-environmental behaviours of the Yangtze Economic Belt .....	62

## List of Tables

Table 1 Major parameters and initial values in the <i>Population Sector</i> .....	12
Table 2 Major parameters and initial values in the <i>Economy Sector</i> .....	14
Table 3 Initial land transfer matrix values (km <sup>2</sup> /year) and total area (km <sup>2</sup> ) .....	16
Table 4 Major parameters and initial values in the <i>Food Sector</i> .....	18
Table 5 Major parameters and initial values in the <i>Energy Sector</i> .....	23
Table 6 Water withdrawal and consumption factors for electricity production .....	26
Table 7 Major parameters and their corresponding values in the <i>Water Sector</i> .....	29
Table 8 Major parameters and their corresponding values in the <i>Carbon Sector</i> .....	32
Table 9 Initial carbon stock and base surface density of NPP values.....	33
Table 10 Parameters of the flow through the terrestrial biosphere.....	33
Table 11 Major parameters and their corresponding values in the <i>Nutrients Sector</i> .....	37
Table 12 Major parameters and their corresponding values in the <i>Fish Sector</i> .....	38
Table 13 Parameters used for the sensitivity test of key state variables in the model.....	41

# 1. INTRODUCTION

## 1.1 Water-Energy-Food Nexus

Today global problems and challenges facing humanity are becoming more and more complex, and directly related to the areas of energy, water, and food production, distribution, and use (Hopwood et al. 2005; Bazilian et al. 2011; Akhtar et al. 2013; van Vuuren et al. 2015; D'Odorico et al. 2018). The relations linking the human race to the biosphere are complex and all aspects affect each other to an extraordinary degree. Therefore, knowledge and methods from a single discipline are no longer sufficient to address these complex, interrelated problems that characterize as fundamental threats to human society anymore (Klein et al. 2001; Bazilian et al. 2011; Clayton and Radcliffe 2018). Researchers and policymakers have promoted the WEF (Water-Energy-Food) nexus approach as a potential framework for addressing sustainability and protecting against risks of future food, water, and energy insecurity (Rasul and Sharma 2016; D'Odorico et al. 2018). The WEF nexus framework was introduced at a conference on "The Water-Energy-Food Security Nexus: Solutions for the Green Economic" in Bonn in 2011. The research and policy-making communities were rapidly attracted by the proposed framework (Daher and Mohtar 2015; Smajgl et al. 2016; Garcia and You, 2016; Weitz et al., 2017; Liu et al. 2017; Xu et al. 2020). The WEF nexus offers a promising approach to identify tradeoffs and synergies of WEF systems and guide the development of cross-sectoral policies. Current applications of the WEF nexus methods, unfortunately, fall short of adequately capturing interactions among the WEF system - the very linkages WEF nexus conceptually aims at addressing (Albrecht et al. 2018; Stoy et al. 2018). Moreover, WEF nexus methods are unable to address the eco-environment dimensions such as biodiversity and ecosystem services and the social-economic dimensions such as population growth and economic development (Kling et al. 2017).

## 1.2 Integrated Assessment Model

Dated back to 1970s, the research supported by the Club of Rome have applied the nexus concept in developing an integrated assessment model to explore *The Limits to Growth* (Meadows et al. 1972). Integrated assessment modelling (IAM), defined as "an interdisciplinary process that combines, interprets, and communicates knowledge from diverse scientific disciplines from the natural and social sciences to investigate and understand causal relationships within and between complicated systems" by the Intergovernmental Panel on Climate Change (IPCC 2001), is widely



adopted to represent complex feedback structures between human and natural systems which evolve. In recent years, as the awareness of climate change and sustainability challenges increase, numerous researchers have dedicated themselves to studying different aspects of global change, aimed at understanding these complex and long-term issues, and to design effective response strategies ([Jakeman and Letcher, 2003](#); [Liu et al. 2007](#); [Davies and Simonovic 2010](#); [Stehfest et al. 2014](#); [Hamilton et al. 2015](#); [Plevin 2017](#); [Zhang and Vesselinov 2017](#); [Calvin et al. 2019](#)). These efforts led to many IAMs with various details in incorporating different system components.

They include the IGSM model (Integrated Global System Model) developed at the Massachusetts Institute of Technology. It includes human activity and emissions, atmospheric dynamics and physics, urban and global atmospheric chemistry, ocean component, and land and vegetation processes ([Prinn et al. 1999](#); [Sokolov et al. 2005](#)).

The IMAGE model (Integrated Model to Assess the Global Environment) developed at Netherlands Environmental Assessment Agency encompasses agricultural economy, forest management, land-use allocation, livestock systems, energy supply and demand, carbon cycle and natural vegetation, crops and grass, water, nutrients, and atmospheric composition and climate ([Stehfest et al. 2014](#)).

The GCAM model (Global Change Analysis Model) developed at the University of Maryland represents five different interacting and interconnected systems: energy, water, land, socioeconomics, and climate ([Calvin et al. 2019](#)).

The ANEMI model developed at the University of Western Ontario represents endogenously the interactions and feedbacks among almost all aspect of human and natural systems, including climate, carbon cycle, population, land use, food production, sea-level rise, hydrologic cycle, water demand, energy-economy, water supply development, nutrient cycles, and persistent pollution ([Davies and Simonovic 2010](#); [Akhtar et al. 2013](#); [Breach 2020](#)).

While these global IAMs provide valuable tools to explore the multiple interactions among human and natural systems and to assess the impacts of global change and adaptation and vulnerability of human society ([Randall et al. 2007](#); [Flato et al. 2013](#)), they are of less value in assisting local and regional policy-making due to their highly aggregated nature ([Holman et al. 2008](#); [Bazilian et al. 2011](#); [Breach 2020](#)). There is an urgent need to find a way to "downscale" global IAMs and apply them at the regional scales to address local-specific challenges ([Breach 2020](#)).

### 1.3 Yangtze Economic Belt Opportunities and Challenges

Originating from the Tanggula Mountains on the Plateau of Tibet and flowing eastward to the East China Sea, Yangtze river is about 6,300 km long with a catchment area of about 1.8 million km<sup>2</sup>. The Yangtze Economic Belt, proposed by the Central Chinese Government in 2016, is set to become yet another essential national-level strategy of China. The Yangtze Economic Belt follows earlier initiatives such as coastal development, western region development, central region development, and Beijing-Tianjin-Hebei integration. Located mainly in the Yangtze river basin, the Yangtze Economic Belt consists of 3 economic zones – the Chongqing-Sichuan upstream urban agglomeration, the central triangle urban agglomeration, and the Yangtze river delta agglomeration, and covers a land area of about 2.05 million km<sup>2</sup>, accounting for 21% of the China's total land area. The Yangtze Economic Belt is home to 40% of the country's total population, with an economic output exceeding 40% of its entire GDP. The relationship between the Yangtze river basin and the Yangtze Economic Belt is illustrated in **Figure 1**.

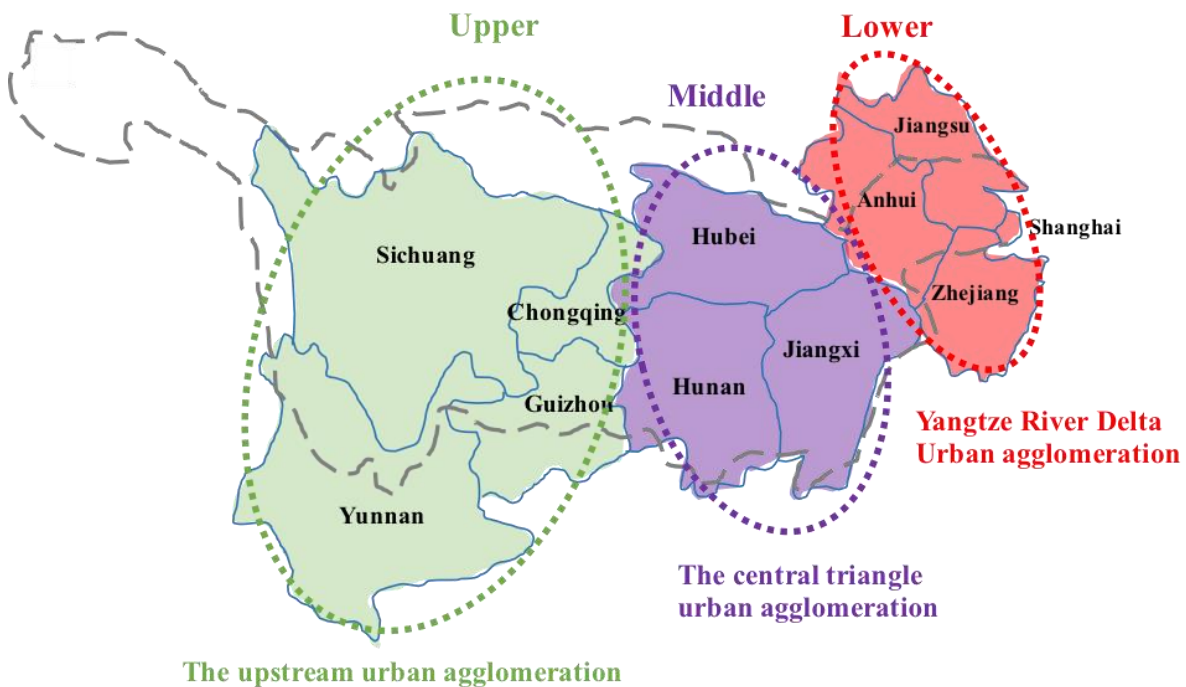


**Figure 1** Yangtze river basin (black dashed line) and the Yangtze Economic Belt

Over the past decades, especially after the reform and opening-up of China in the late 1970s, the Yangtze river basin has developed into one of the strongest regions in China. The Yangtze

Economic Belt has unique economic advantages and huge development potential in terms of geographic location, water resources, and its comprehensive industrial infrastructure. Yangtze Economic Belt traverses eastern, central and western China, joining the coast with the inland. The Yangtze Economic Belt's intensive railway, highway, and aviation transportation systems link east to west and connect south to north, making the movement of goods and services more efficient. In addition, the Yangtze Golden Waterway, which ranks first among inland rivers in the world in terms of transport volume, also provides competitive low water transport cost and low power consumption. Yangtze river basin has abundant freshwater resources, and Yangtze's average annual discharge into the East China Sea is about 905 km<sup>3</sup>/year (Yang et al. 2015). Yangtze Economic Belt is one of the most important industrial corridors in China. It is home to many advanced manufacturing industries, modern service industries, major national infrastructure projects, and high-tech industrial parks.

However, the fast development of urbanization and economic growth in the Yangtze Economic Belt pose severe challenges for its sustainable development. Yangtze river basin is very poor in fossil fuel endowments (Wang et al. 2020). Most of its energy is imported from other parts of China and abroad. The growth of population and urban expansion occupy many rich farmlands, thus threatening food security (Cai and Fangyuan 2020). The increasing application of fertilizers and pesticides, and municipal waste from a growing population and the rapid development of industry lead to serious water pollution (Wong et al., 2007; Li et al., 2009; Xu et al., 2010; Li et al. 2011; Xia et al. 2016). Also, the fishery resources in the Yangtze river are so seriously depleted that the government issued a 10-year commercial fishing ban on the Yangtze river in 2020 (Zhang et al. 2020). These challenges tend to further deteriorate under the climate change.

## 2. ANEMI\_YANGTZE MODEL FRAMEWORK AND CROSS-SECTORAL FEEDBACKS

ANEMI\_Yangtze, which is "downscaled" from ANEMI, is an integrated assessment model developed particularly for the Yangtze Economic Belt in China. Unlike the ANEMI model, in ANEMI\_Yangtze, hydrological cycle, water demand and water supply development, as well as wastewater discharge and treatment, are all part of a *Water Sector*. Climate change is not part of the model. Instead, we use exogenous precipitation and temperature data for the Yangtze river basin to drive the *Water Sector's* hydrological cycle. Sea level rise and persistent pollution sectors are not included either. The global cycles of carbon, nutrients, and hydrology are tailored to fit a regional context. Some major modifications are to be seen in the *Population, Food, and Energy Sectors*. Their details are presented in the following sections of the report. A new sector of fish population is added into ANEMI\_Yangtze to address the fish depletion issues in the Yangtze river. The model sectors that comprise the ANEMI\_Yangtze include population, economy, land, food, energy, water, carbon, nutrients, and fish.

### 2.1 Framework of ANEMI\_Yangtze

The architecture of ANEMI\_Yangtze model consists of three layers, the upper policy layer, the middle socio-economic and natural-environmental interacting layer, and the lower impacts assessment layer. They are illustrated in **Figure 2**. In the policy layer, different policies regarding population growth, land-use transfer, energy development, water use, and eco-environmental improvement are proposed. They act directly on the social-economic system, natural resources system, and eco-environmental system. The systems interacting layer captures the interactions among the population, economy, land cover and land use, food, energy, water, carbon, nutrients, and fish subsystems. In the impacts layer, the *GDP per capita, food self-sufficiency, energy deficit, water stress, nutrients concentration, carbon emissions, and fish yield* are assessed.

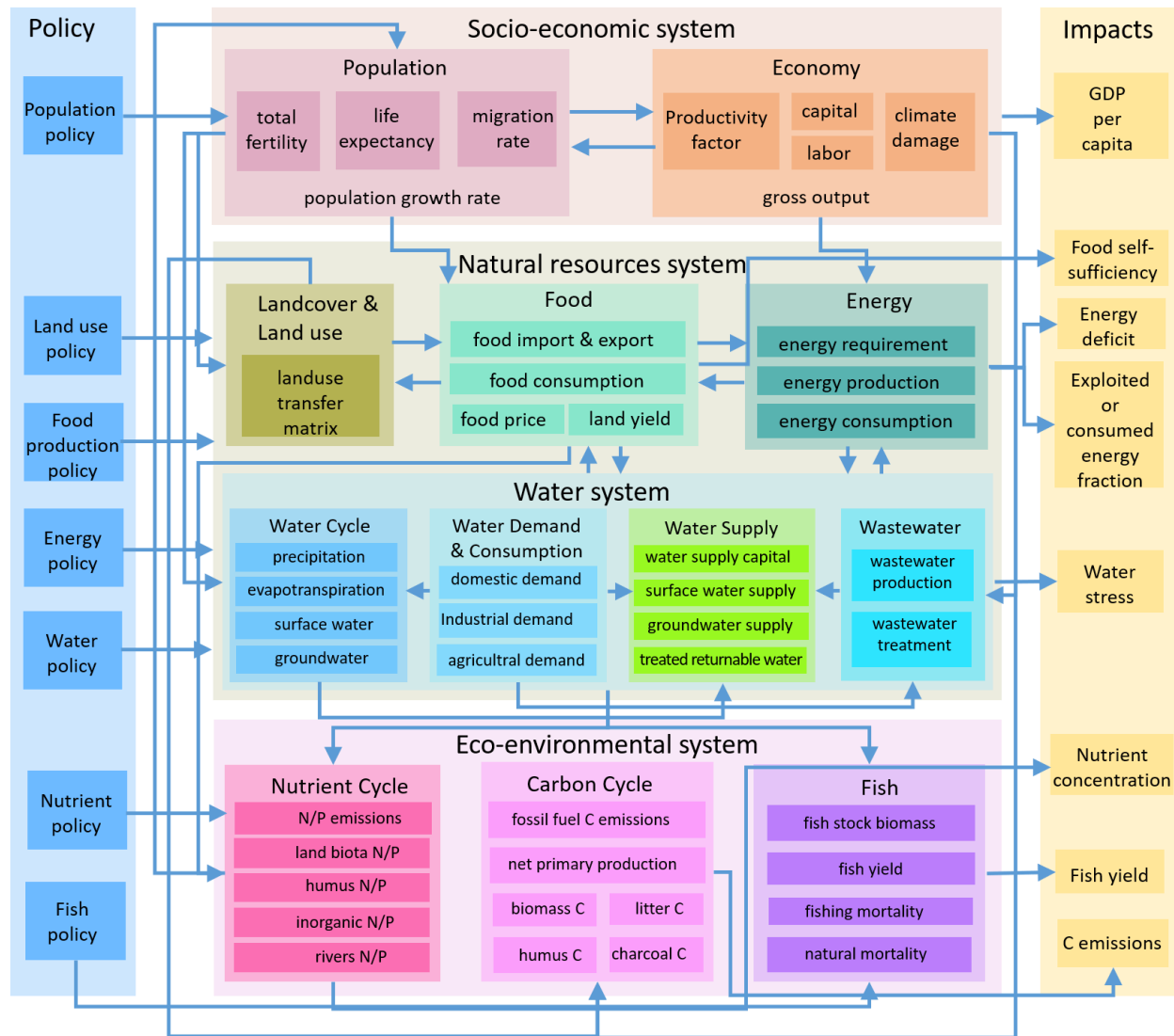


Figure 2 Framework of the ANEMI\_Yangtze model

## 2.2 Cross-sectoral Feedbacks in ANEMI\_Yangtze

This section presents the cross-sectoral interactions and feedbacks in the ANEMI\_Yangtze model. The major interactions and feedbacks between the subsystems in human-natural systems in ANEMI, which are responsible for the functioning of the Earth system, are also applicable to the Yangtze Economic Belt in this research. Unlike the global human-natural system, the human-nature system in Yangtze Economic Belt undergoes constant exchange of goods and services with the outside world through market trade and migrations. So, some exogenous drivers are also significant for the ANEMI\_Yangtze model. Even though the ANEMI\_Yangtze model is not that highly endogenous like its parent model ANEMI, there is no doubt that it is the feedback processes

among the various subsectors of the Yangtze Economic Belt system that drive the dynamic behaviours exhibited in the model runs. In the following section, the cross-sectoral interactions and feedbacks in ANEMI\_Yangtze (**Figure 3**) were discussed.

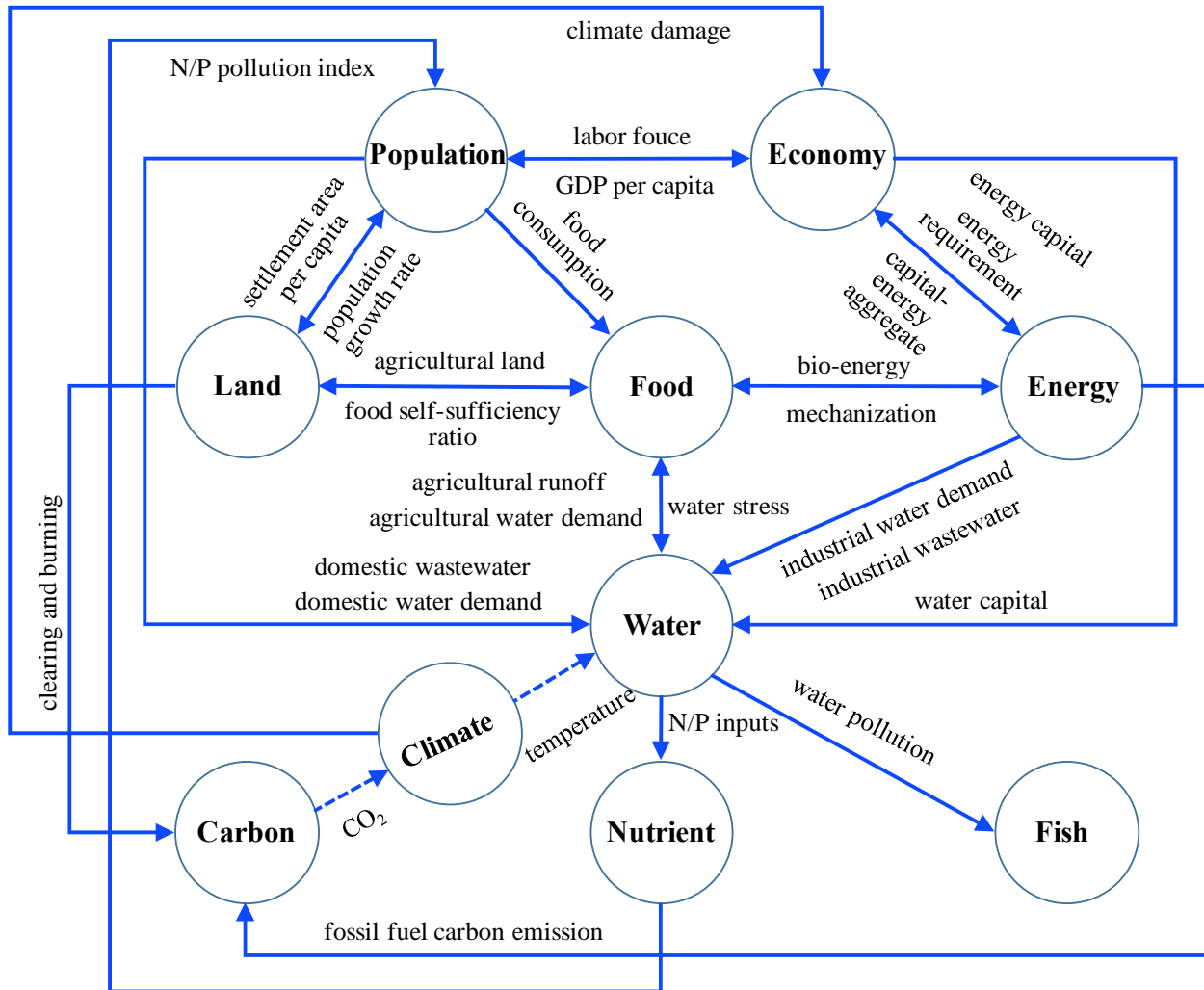


Figure 3 Interactions among the human-natural systems in the Yangtze Economic Belt

The *Population Sector* affects the *Economy Sector* positively by boosting the *labour force* and is affected by the *Economy Sector* both positively and negatively through *GDP per capita*. On the one hand, an increase in *GDP per capita* increases the *health service output*, which has a positive effect on *life expectancy* and thus reduces the death rate of the *population*. On the other hand, an increase in *GDP per capita* has the opposite effect on the *desired family size*, affecting *total fertility* and thus reducing the birth rate of the *population*. The difference of *GDP per capita* between

Yangtze Economic Belt and the rest of China also affects population migration. Usually, people tend to migrate from less developed regions to more developed regions.

The *Population, Food, and Land Sectors* are connected through *population growth rate, food self-sufficiency ratio, and settlement area per capita*. The population growth accelerates the transfer rate of biome among different land-use types. Population growth drives *food consumption*, thereby decreasing *food self-sufficiency*, resulting in more agricultural land being converted from clearing and burning forest and grassland. The population growth also leads to more agricultural land around the urban area be claimed for settlement use as urbanization expands. The *Land Sector* can act as negative feedback on population growth as increased population places more stress on *settlement area per capita*. The stress on settlement area then acts as an opposing force on the migration rate.

The *Economy and Energy Sectors* are linked through *capital-energy aggregate, energy capital, and energy requirement*. A growing economy increases the requirement for energy, which drives *energy production* through the increasing investment of *energy capital*. An increase in *energy capital* further intensifies the *capital-energy aggregate*, leading to the growth of the economy, thus forming a positive feedback loop.

The *Population, Food, Energy, and Water Sectors* are connected via domestic water demand and consumption, agricultural water demand and consumption, and industrial water demand and consumption. Water (irrigation) plays a vital role in food production. Water is needed in almost every stage of energy extraction, production, processing, and especially the consumption. With increased population and demand for food and energy, the total demand for and consumption of water increases, increasing water stress. Water stress, in turn, has a limiting effect on population growth and food production. The increase in water stress also drives more capital flowing into water supply development to alleviate water stress, thus connecting the *Economy* sector with the *Water Sector*.

The use of water by *Population, Food, and Energy Sectors* all result in water pollution in the form of nitrogen (N) and phosphorus (P) through the discharge of domestic and industrial wastewater and agricultural runoff. This links the *Water Sector* with the *Nutrient Sector*. An increased level of *nutrients concentration* negatively affects population growth through the *life expectancy*

*multiplier* from the N/P pollution index. Water pollution also endangers the fish by increasing the fish's natural mortality rate.

The *Carbon* and *Land Sectors* are connected through clearing and burning, while the *Carbon* and *Energy Sectors* are connected through fossil fuel emissions. The *Carbon-Climate* sector feedback depends on the atmospheric CO<sub>2</sub> concentration determined by the *Carbon* sector. As carbon and climate interactions usually happen at the global scale, for the Yangtze Economic Belt these two sector interactions are not considered. The climate change effect is treated as exogenous input. The *Climate* and *Water Sectors* are connected via the surface temperature change. Since increased surface temperature will likely increase the intensity of the hydrological cycle, the model includes a temperature multiplier equation that increases evaporation and evapotranspiration within the Yangtze hydrological cycle. The *Climate Sector* influences the *Economy* sector through a temperature damage function.



### 3. ANEMI\_YANGTZE MODEL STRUCTURE DESCRIPTION

The cross-sectoral interactions and feedbacks are responsible for the functioning of the whole human-nature system in the Yangtze Economic Belt. For each sector in the ANEMI\_Yangtze model, the relevant feedbacks drive the dynamics of state variables in the sector. This chapter illustrates the causal feedbacks within each sector and provides the general description of the ANEMI\_Yangtze model sectors.

#### 3.1 Population Sector

The causal loop diagram in **Figure 4** illustrates the feedbacks associated with the *Population Sector* in the Yangtze Economic Belt. The three variables - *births*, *deaths*, and *migrants*, which are all affected by *GDP per capita*, drive the dynamic behaviour of the *population*. The *Population Sector* is affected by *Land Sector*, *Water Sector*, and *Energy Sector*. The increase of *population* on one hand, decreases the value of *GDP per capita* as the *population* is a denominator. On the other hand, the rise in population boosts the *labour force*, and thus the *gross output* as economic output is represented as a function of capital and labour in the form of a Cobb-Douglas production function. The increase of the *gross output* eventually increases the value of *GDP per capita*. Overall, *GDP per capita* increases if the effect of the increase in the *gross output* outpaces the effect of increase in population, and vice versa. This means all the feedback loops containing *GDP per capita* can either be positive or negative depending on whether *GDP per capita* is increasing or decreasing with population growth (for example, the B1 and C1 loops in **Figure 4**).

An increase in *GDP per capita* on the one hand, means more inputs in health services, thus improves *life expectancy* and lowers the mortality rate. A decrease in mortality means fewer *deaths*, which drives the *population* to grow. On the other hand, an increase in *GDP per capita* leads to a decrease in the willingness to give birth, which will drive the population to decline. Migration is newly added. Usually, people migrate from poor regions to rich regions within China. In this research, migration behaviour is mainly driven by a variable named *GDP difference factor*, which is used to calculate the difference between *national GDP per capita* and the *GDP per capita* in the Yangtze Economic Belt. Besides, the effect of the crowding is also taken into account, which acts as negative feedback on migration. On the global scale, water and food availability usually act as limits to population growth. At the regional scale, vital resources such as food and water can be traded, so in ANEMI\_Yangtze, only the effect of pollution on the population is taken into account.

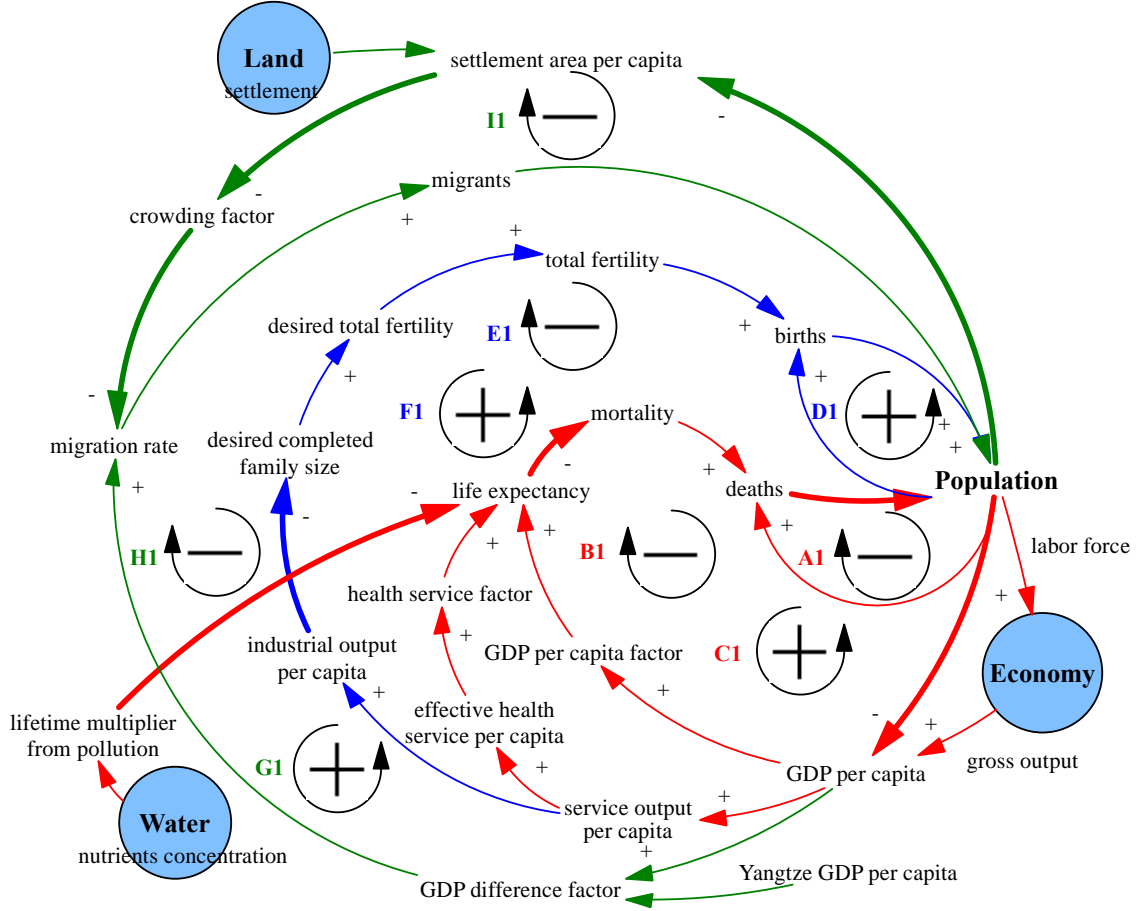


Figure 4 Causal feedback loops of the *Population Sector*

The ageing chain of population groups can be represented as,

$$P_{0-14} = \int (births + netM_{0-14} - P_{0-14} \cdot M_{0-14} - \frac{P_{0-14}(1-M_{0-14})}{\tau_1}) dt \quad (1)$$

$$P_{15-64} = \int (netM_{15-64} + \frac{P_{0-14}(1-M_{0-14})}{\tau_1} - P_{15-64} \cdot M_{15-64} - \frac{P_{15-64}(1-M_{15-64})}{\tau_2}) dt \quad (2)$$

$$P_{65+} = \int (netM_{65+} + \frac{P_{15-64}(1-M_{15-64})}{\tau_2} - P_{65+} \cdot M_{65+}) dt \quad (3)$$

where  $P_i$  = population,  $netM_i$  = net migrations,  $M_i$  = mortality rate,  $\tau_i$  = length of time spent in sub-demographic.

The *total fertility*, *life expectancy*, and *migration rate* are calculated by the following formulas,

$$TF = MIN(MTF, (MTF \cdot (1 - F_{control}) + DTF \cdot F_{control})) \quad (4)$$

$$LE = (LE_{normal} + F_{GDP/capita} + F_{health}) \cdot Pollution_{multi} \quad (5)$$

$$MR = F_{GDP\ diff} \cdot MW \cdot MP \cdot F_{crowding} \quad (6)$$

where  $TF$  = total fertility,  $MTF$  = maximum total fertility,  $F_{control}$  = fertility control effectiveness,  $DTF$  = desired total fertility,  $LE$  = life expectancy,  $LE_{normal}$  = life expectancy normal,  $F_{GDP/capita}$  = GDP per capita factor,  $F_{health}$  = health service factor,  $Pollution_{multi}$  = lifetime multiplier from pollution,  $MR$  = migration rate,  $F_{GDP\ diff}$  = GDP difference factor,  $MW$  = migration willingness,  $MP$  = migration policy,  $F_{crowding}$  = crowding factor.

Some of the major parameters and initial values in the *Population Sector* are provided in **Table 1**.

Table 1 Major parameters and initial values in the *Population Sector*

Population 0-14 (10 <sup>4</sup> person)	Population 15-64 (10 <sup>4</sup> person)	Population 65+ (10 <sup>4</sup> person)	Life expectancy normal (year)	Reproductive lifetime	Female ratio
13457	34275	3106	52.5	35	0.5

### 3.2 *Economy Sector*

The *Economy Sector*, which is developed and adjusted based on the FREE model from [Fiddaman \(1997\)](#), computes the *gross output* of the Yangtze Economic Belt. The *gross output* is represented as a function of *capital* and *labour* in the form of a Cobb-Douglas production function (see supplemental materials for calculation details). The *Economy Sector* is affected by *Population Sector* and *Energy Sector*.

The interactions and feedbacks in the *Economy Sector* are diagrammed in **Figure 5**. The A2 and B2 feedback loops depict the adjustment of *desired capital* in response to relative cost and *marginal productivity of capital*. The C2 feedback loop corrects the gap between *desired capital* and actual *capital*. The D2 feedback loop illustrates the effect of the *expected output growth rate* on *desired capital order rate*. The E2 and F2 feedback loops illustrate *capital* depreciation into investment in additional *capital*.

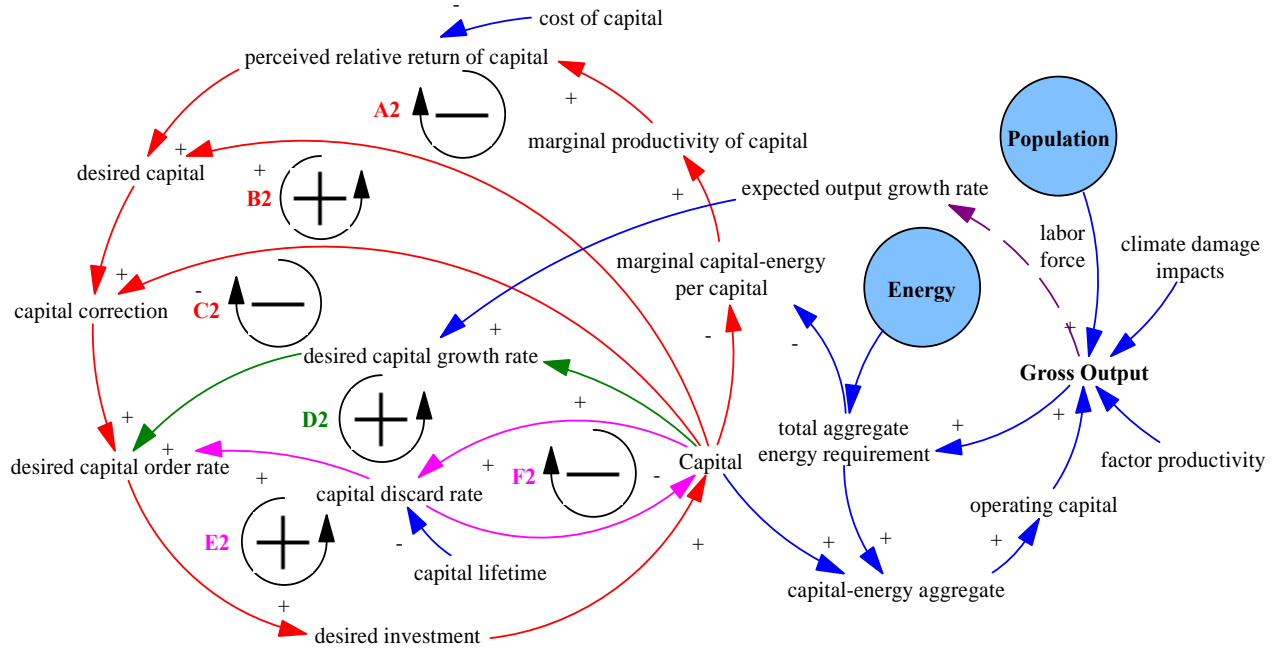


Figure 5 Causal feedback loops of the economy sector

*Gross output* is determined using a Cobb-Douglas production function in the following form,

$$Y = Y_0 A_t \left(\frac{L}{L_0}\right)^\alpha \left(\frac{KO}{KO_0}\right)^{(1-\alpha)} \quad (7)$$

where,  $Y$  = gross output,  $L$  = labour force,  $KO$  = operating capital,  $A_t$  = factor productivity,  $\alpha$  = value share of labour,  $Y_0$  = gross output,  $L_0$  = labour force,  $KO_0$  = operating capital.

*Capital* stock for the production of goods increases with investment and decreases with depreciation, which is a fixed fraction of capital,

$$K(t) = \int (I - \delta K) dt \quad (8)$$

where,  $K$  = capital,  $I$  = capital investment rate,  $\delta$  = fractional depreciation rate.

The *capital investment* equation takes the following form,

$$I = \delta K + \frac{(K_D - K)}{\tau_K} + KG \quad (9)$$

where  $K_D$  = desired capital,  $\tau_K$  = capital correction time,  $G$  = fractional growth rate of output. *Desired capital* equals to the current level of capital adjusted for the relative cost and marginal product of capital and is defined as,

$$K_D = \frac{KM_K}{r+1/\tau} \quad (10)$$

where  $M_K$  = marginal product of capital,  $r$  = interest rate,  $\tau$  = capital lifetime.

Some of the major parameters and initial values in the *Economy Sector* are provided in **Table 2**.

Table 2 Major parameters and initial values in the *Economy Sector*

Variable	Value	Unit	Definition
reference capital	1.657e+11	¥	Reference capital stock (capital stock in 1990)
reference output	7.21292e+11	¥	Reference goods output (GDP in 1990)
capital lifetime	40	year	Lifetime of goods producing capital.
output trend time	15	year	Time to establish long-term trend in output for capital planning.
interest rate	0.09	1/year	Constant exogenous interest rate.
hist output growth rate	0.2	1/year	Historic growth rate of output and investment.
capital energy substitution elasticity	0.75	dmnl	Elasticity of substitution between capital aggregate energy good in capital-energy aggregate.
value share of labour	0.6	Dmnl	Cobb-Douglas value share of labour in output.

### 3.3 Land Sector

The *Land Sector* is used to describe the distribution of land use and cover over time. It is adapted from ANEMI (Davies 2007; Breach 2020), which was originally based on the model of Goudriaan and Ketner (1984). What's different from ANEMI, is that in ANEMI\_Yangtze land cover classes are grouped into the six IPCC land categories, *i.e.* agricultural land (cropland), forest, grassland,

wetland, settlement, and other land. There is no feedback loop within the *Land Sector*. A transfer matrix is adopted to depict the change rate at which one land cover type changes into another, driven by the population growth rate. Please refer to the supplementary materials for calculation details.

The *land transfer rate* is represented as,

$$L_{trans} = L_{tm} \cdot r \quad (11)$$

where  $L_{tm} = \text{Transfer Matrix}$  [km<sup>2</sup>/year],  $r = \text{population growth rate}$  [1/year].

The *land transfer matrix* works as a reservoir where inflow is *land transfer rate* and outflow is *drain transfer value* ( $L_{idr}$ ), which is used in the model to avoid any negative term. The calculation of *transfer matrix* is as follows,

$$L_{tm} = \int (L_{trans} - L_{idr}) \cdot dt \quad (12)$$

The *land transfer matrix* is used to drive the change in biome area at a rate equal to the sum of the transfer rates from biome  $i$  to biome  $j$ , minus the sum of transfer rates from biome  $j$  to biome  $i$ ,

$$\frac{dA_j}{dt} = \sum_{i=1}^6 a_{ij} - a_{ji} \quad (13)$$

where  $A_j = \text{current area of biome } j$  [km<sup>2</sup>],  $a_{ij} = \text{rate of transition of area from biome } i \text{ to biome } j$  [km<sup>2</sup>/year].

The initial *land transfer matrix* and *initial biome area* are shown in **Table 3**. These initial transfer values were obtained by averaging the transfer that happened from 1992 to 2015. The matrix values in the table can be interpreted as the rate of transfer from the biome type in row  $i$  to the biome type in column  $j$ . The non-diagonal elements are the base land transfer rates from one biome type to another. The diagonal elements are zero, indicating there are no shifts within a same biome.

Table 3 Initial land transfer matrix values (km<sup>2</sup>/year) and total area (km<sup>2</sup>)

From \ To	agriculture	forest	grassland	wetland	settlement	other
agriculture	0	812.24	42.35	2.52	934.3	72.96
forest	2050.41	0	74.82	5.26	34.58	32.37
grassland	196.03	296.7	0	0.63	107.36	6.46
wetland	1.14	0.89	0.14	0	3.53	4.36
settlement	6	0.04	0.18	0.01	0	0.58
other	261.3	634.43	23.64	48.7	13.91	0
1990 area	1019225	798327	202956	6925	9097	64489

### 3.4 Food Sector

The *Food Sector* in ANEMI\_Yangtze is quite different from the *Food Sector* of ANEMI. In China, *food self-sufficiency* is an essential index. The country manages to keep its value at 0.95 in order to maintain food security. In ANEMI\_Yangtze, the dynamic behaviour of *food production* is mainly driven by the difference between perceived *food self-sufficiency* and *desired food self-sufficiency* which serves as an indicator for land yield technology input and fertilizer subsidy. The food sector also enables the trade of food, *i.e.*, *food import* and *food export* (which is affected both by local food price and international price). The import and export of food affect the *food stock* and the *food price*. The *food price change* is another factor affecting *food production*. An increase in *food price change* acts as positive feedback on farmers' adopting of multiple cropping practices (*multiple cropping index*) and increasing *grain planting area*.

The production of food is affected by several factors, including *land fertility*, *arable land*, and *water stress*. The *Food Sector* is affected by *Population Sector*, *Land Sector*, and *Water Sector*. The feedback loops of the *Food Sector* are shown in **Figure 6**. Loops A3, B3, and C3 illustrate the impacts of *land yield technology*, *agricultural land development*, and *fertilizer subsidy*, respectively, on food production through the indicator of *food self-sufficiency ratio*. Loops D3, E3, and F3 depict the introduction of multiple cropping practices (*multiple cropping index*) and *willingness to increase grain planting area* on food production through *food price change*.

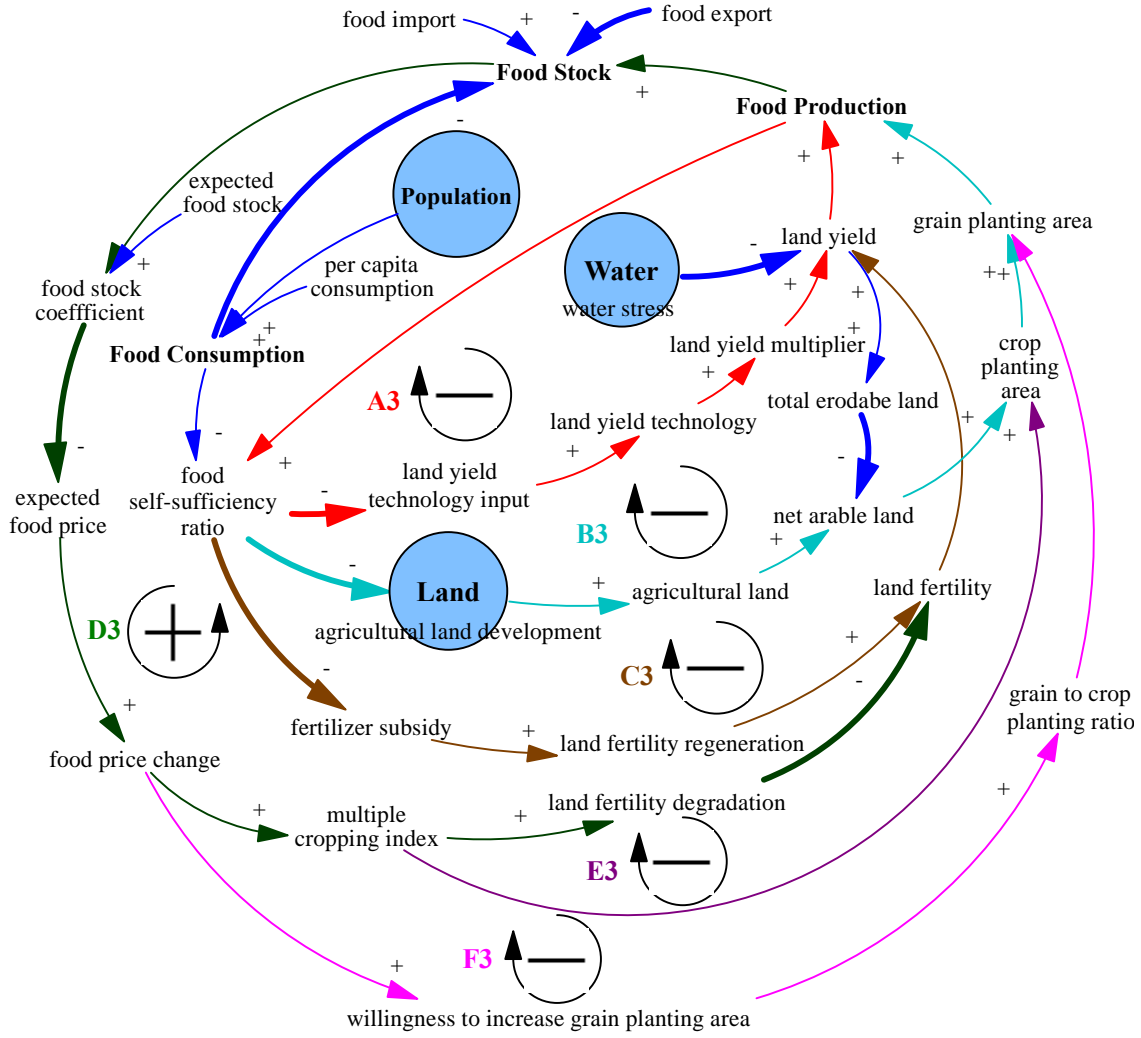


Figure 6 Causal feedback loops of the food sector

Main equations in the *Food Sector* are given in the following:

$$LY = LF \cdot LY_{multi} \cdot F_{WS} \quad (14)$$

$$FP = LY \cdot GPA \cdot LFH \cdot (1 - Loss) \quad (15)$$

$$FIE = F_{pop} \cdot f_1 + f_2 \cdot FP - f_3 \cdot ICP \quad (16)$$

$$FC = P \cdot FC_{per\ capita} \quad (17)$$

$$R_{fsc} = \frac{FP}{FC} \quad (18)$$

where  $LY$  = land yield,  $LF$  = land fertility,  $LY_{multi}$  = land yield multiplier,  $F_{WS}$  = water stress to land yield factor,  $FP$  = food production,  $GPA$  = grain planting area,  $LFH$  = land fraction harvested,  $Loss$  = processing loss,  $FIE$  = food import/export,  $F_{pop}$  = population rescale factor,  $f_i$  = constant



factors,  $FP$  = food price,  $ICP$  = international cereal price,  $FC$  = food consumption,  $P$  = population,  $FC_{per\ capita}$  = per capita food consumption,  $R_{fsc}$  = food self-sufficiency ratio,  $FP$  = food production.

Some of the major parameters and initial values in the *Food Sector* are provided in **Table 4**.

Table 4 Major parameters and initial values in the *Food Sector*

Variable	Value	Unit	Note
inherent land fertility	6300	kg/hectare	
initial land fertility	4800	kg/hectare	
desired food self-sufficiency ratio	0.95	dmnl	
normal cropping index	1.3	dmnl	
normal grain-crop ratio	0.65	dmnl	The ratio of grain planting area to crop planting area.
processing loss	0.01	dmnl	
average life of land normal	6000	year	
initial yield tech	1	dmnl	
initial stock	18500	10 <sup>4</sup> tonne	Initial food stock
per capita food consumption	400	kg/person/year	

### 3.5 Energy Sector

The *Energy Sector* consists of *energy requirement*, *energy capital*, and *energy production*. In ANEMI\_Yangtze, the *total aggregate energy requirement* is calculated based on the economic output multiplied by the *energy consumption per unit GDP* whereas in ANEMI the *energy requirement* is embodied in capital. The *energy requirement* of different energy sources (coal, oil, gas, hydropower, nuclear, new energy sources) is the product of *total aggregate energy requirement* and *desired energy share* (which is treated as an exogenous variable). *Energy capital* for different energy sources is structured in a similar way to that of the *capital stock* in the *Economy Sector*. The significant difference is that there is a stock representing *energy capital under construction* which after a delay time becomes new *energy capital*. The production of energy is

determined by the amount of *capital* stock accumulated into each energy source and is influenced by production pressures. Limitations on *energy production* are in the form of depletion for nonrenewable energy sources (coal, oil, gas) and saturation for renewable energy sources (hydropower, nuclear, new energy sources).

The feedback loops in the *Energy Sector* are seen in **Figure 7**. In which, feedback loop A4 depicts the process of *energy capital* depreciation, which slowly depletes the *energy capital* stock. Loop B4 compensates for depreciation by factoring it into *desired energy capital under construction*. Loop C4 moves *energy capital* from the construction phase to the completion phase. Loops D4 and E4 depict the effect of *energy production* pressure on *energy capital*. Loop F4 illustrates the impact of resource depletion on *energy production*. Energy resources gradually deplete as more energy is produced. This affects the ratio of *energy resources remaining*, which acts as a negative factor on *energy production*, creating a negative feedback loop. Loop G4, together with Loop E4 illustrate the impact of *effective energy capital input effect* on energy production through *energy technology* and *energy capital*, respectively. *Energy technology* plays a role in the production of energy through cumulative energy investment, which acts to increase *energy production* for the same level of inputs of capital. Loop H4 depicts the effect of *energy technology* on energy consumption intensity per unit GDP.

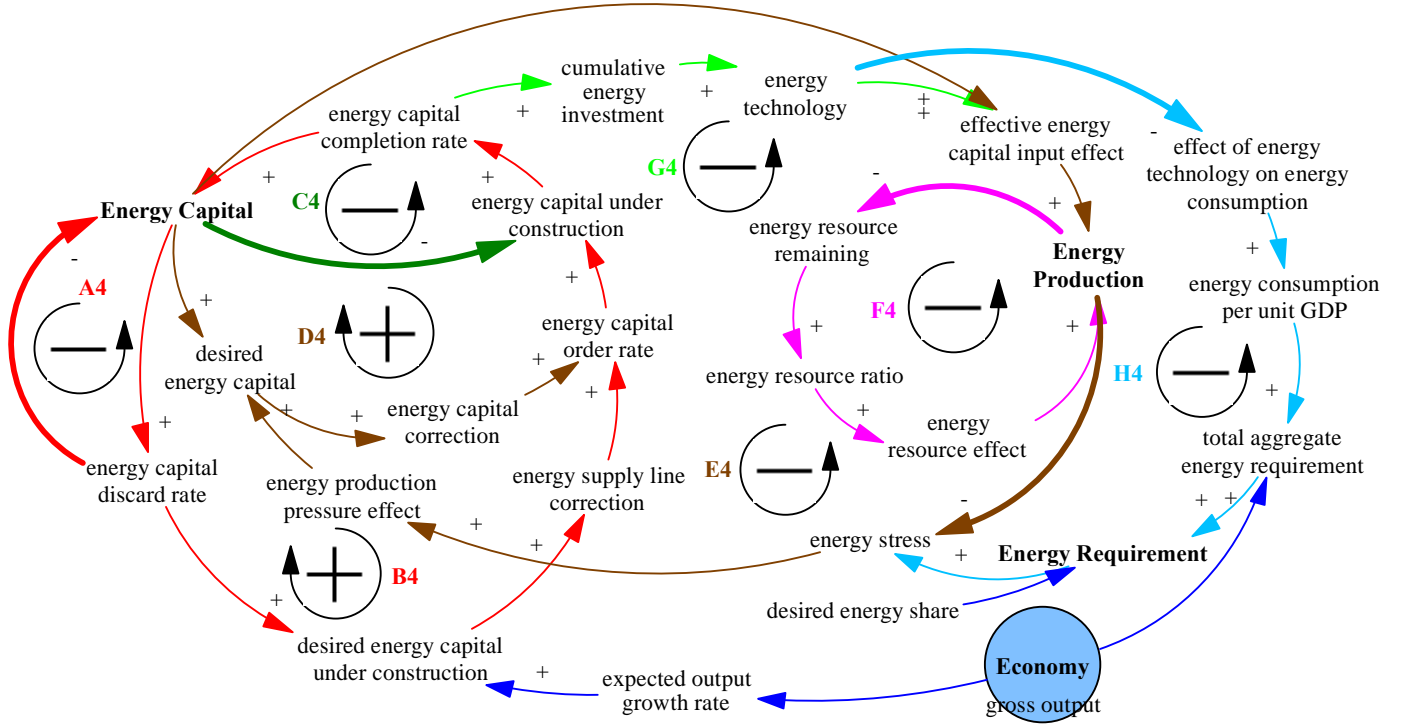


Figure 7 Causal feedback loops of the *Energy Sector*

The *energy capital* stock can be represented mathematically by,

$$KE_i(t) = \int \left( \frac{KC_i}{\tau_c} - \frac{KE_i}{\delta_i} \right) dt \quad (19)$$

where  $KE_i$  = energy capital for energy source  $i$ ,  $KC_i$  = energy capital under construction for energy source  $i$ ,  $\tau_c$  = capital construction delay,  $\delta_i$  = energy capital lifetime,

$$KC_i(t) = \int \left( EKO_i - \frac{KC_i}{\tau_c} \right) dt \quad (20)$$

where  $EKO_i$  = energy capital order rate.

The *energy capital order rate* is formulated in the same way as the *capital investment rate*. It compensates for *capital* depreciation, adjusts for perceived growth in energy orders, and responds to discrepancies in desired versus current *energy capital* stock,

$$EKO_i = \frac{KE_i}{\delta_i} + \frac{DKE_i - KE_i}{\tau_K} + \frac{DKC_i - KC_i}{\tau_{KC}} \quad (21)$$

where  $DKE_i$  = desired energy capital,  $DKC_i$  = desired energy capital under construction,  $\tau_{KC}$  = time to correct capital construction,

$$DKE_i = KE_i \times EP_i \quad (22)$$

where  $EP_i$  = energy pressure effect for energy source  $I$ ,

$$DKC_i = KE_i(\delta_i + G)\tau_C \quad (23)$$

The equation of *energy production* takes the following form,

$$EP_i = EP_{i,0}(\alpha_i(\frac{R_i}{R_{i,0}})^{\rho_i} + (1 - \alpha_i)EII_i^{\rho_i})^{\frac{1}{\rho_i}} \quad (24)$$

where  $EP_i$  = energy production,  $EP_{i,0}$  = initial energy production,  $\alpha_i$  = energy resource share,  $R_i$  = energy resource remaining,  $R_{i,0}$  = initial energy resource remaining,  $\rho_i$  = energy resource substitution coefficient,  $EII_i$  = energy effective input intensity.

The *energy resource share* provides an upper limit on energy production by representing the minimum time required for resource extraction in the case of nonrenewables, and the maximum resource flux in the case of renewables.,

$$\alpha_{nonrenewable} = (\frac{R_{i,0}}{\tau_r EP_{i,0}})^{\rho_{nonrenewable}} \quad \alpha_{renewable} = (\frac{R_{i,0}}{EP_{i,0}})^{\rho_{renewable}} \quad (25)$$

where  $\tau_r$  is the minimum resource depletion time in years. As energy resources are consumed, for example, in the case of fossil fuels, there is a depletion effect that acts to decrease energy production. The energy effective input intensity depends on the level of *energy technology* development as well as *energy capital* inputs put into production and it takes the following form,

$$EII_i = TE_i \left( \frac{KE_i}{KE_{i,0}} \right)^{\beta_i} (V_{relative,i})^{(1-\beta_i)} \quad (26)$$

where  $TE_i$  = energy technology for energy source  $i$ ,  $KE_i$  = energy capital for energy source  $i$ ,  $KE_{i,0}$  = initial energy capital for energy source  $i$ ,  $\beta_i$  = energy capital share for energy source  $i$ ,  $V_{relative,i}$  = relative variable energy intensity for energy source  $i$ .

Aggregate energy requirement intensity, *i.e.*, *aggregate energy consumption per unit GDP*, is used to predict the *total aggregate energy requirement*. Aggregate energy requirement intensity is calculated by the reference aggregate energy intensity adjusted by the effect of *energy technology* on energy consumption and takes the following form,

$$ERI_{aggr} = ERI_{aggr,0} \cdot f_{TE} \quad (27)$$

where  $ERI_{aggr}$  = aggregate energy requirement intensity,  $ERI_{aggr,0}$  = initial aggregate energy requirement intensity,  $f_{TE}$  = effect of energy technology on energy consumption. The requirement of each energy resource is then equals to the production of gross output and aggregate energy requirement intensity multiplied by the desired energy share for each energy source,

$$ER_i = \gamma_{desire,i} Y \cdot ERI \quad (28)$$

where  $\gamma_{desire,i}$  is the exogenous desired energy share for each energy source.

Some of the major parameters and initial values in the *Energy Sector* are provided in **Table 5**.

Table 5 Major parameters and initial values in the *Energy Sector*

Variable	Value	Unit
energy resource elasticity [coal, oil, gas, hydro, nuclear, new]	0.625276, 0.6573, 0.6573, 0.302451, 0.302451, 0.527352	Dmnl
energy capital share [coal, oil, gas, hydro, nuclear, new]	0.6, 2/3, 2/3, 0.8, 0.8, 0.8	Dmnl
energy capital lifetime [energy source]	15, 15, 15, 30, 30, 20	year
energy construction delay	2	year
supply line correction time	4	year
initial energy production [coal, oil, gas, hydro, nuclear, new]	1.73453e+08, 2.7027e+06, 8.802e+06, 8.52e+06, 1, 1.08e+06	tce/year
ref energy consumption per unit GDP	6	tce/10 <sup>4</sup> ¥

### 3.6 Water Sector

The hydrological cycle in the Yangtze Economic Belt describes the flow of water from the atmosphere in the form of *precipitation* to the land *surface storage* and through the *groundwater* back to the East China Sea. The *surface storage* and *groundwater* are treated as a kind of reservoir from which water flows to and from. *Water demand* is the sum of the desired water withdrawals from agricultural, domestic, and industrial sectors. *Domestic water withdrawal* depends on structural water intensity related to GDP to withdrawal rate per person based on the conceptual model presented in [Alcamo et al. \(2003\)](#). The generation of electricity typically dominates water withdrawals in the industrial sector. In ANEMI\_Yangtze, electricity production consists of both nonrenewable sources (coal-fired and gas-fired thermal power) and renewable sources (hydropower and nuclear power). The water withdrawal factor and water consumption of thermal energy vary substantially among different cooling methods. The nuclear power in the Yangtze Economic Belt only withdraws seawater, so the freshwater withdrawal and consumption factors of nuclear power are all set to zero. *Agricultural water demand* is the production of *per hectare water withdrawal* and *net arable land*. Changes in surface temperature are also included as additional factors affecting water demand for food production. The *water supply* in ANEMI\_Yangtze is quite different from that in the ANEMI. In ANEMI\_Yangtze, three supply

types are considered by adding capital stocks to produce *water supply* in the form of surface, ground, and wastewater reclamation water sources. The production of water supplies is driven economically by investing in capital stocks for each source. *Water stress* is used as an indicator for water capital investment.

The causal loops in the *Water Sector* are illustrated in the causal loop diagram in **Figure 8**. Feedback loop A5 acts as negative feedback on *water supply capital* through depreciation. Loop B5 counteracts the A5 by having a positive feedback effect on *water supply capital*. With more *water supply capital*, there is more depreciation, which increases the *water capital order rate* (investment in the water supply), thus adding more *water supply capital*. Loops C5, D5, and E5 counteract *water stress* by prompting investment in *water supply capital* to increase water supplies in the form of *surface water*, *groundwater*, and *treated returnable waters*, respectively. Feedback loop F5 illustrates the movement of water from the atmosphere to the surface as *precipitation* and then back to the atmosphere through *evapotranspiration*. Loop H5 depicts the effect of *discharge* on *groundwater*.

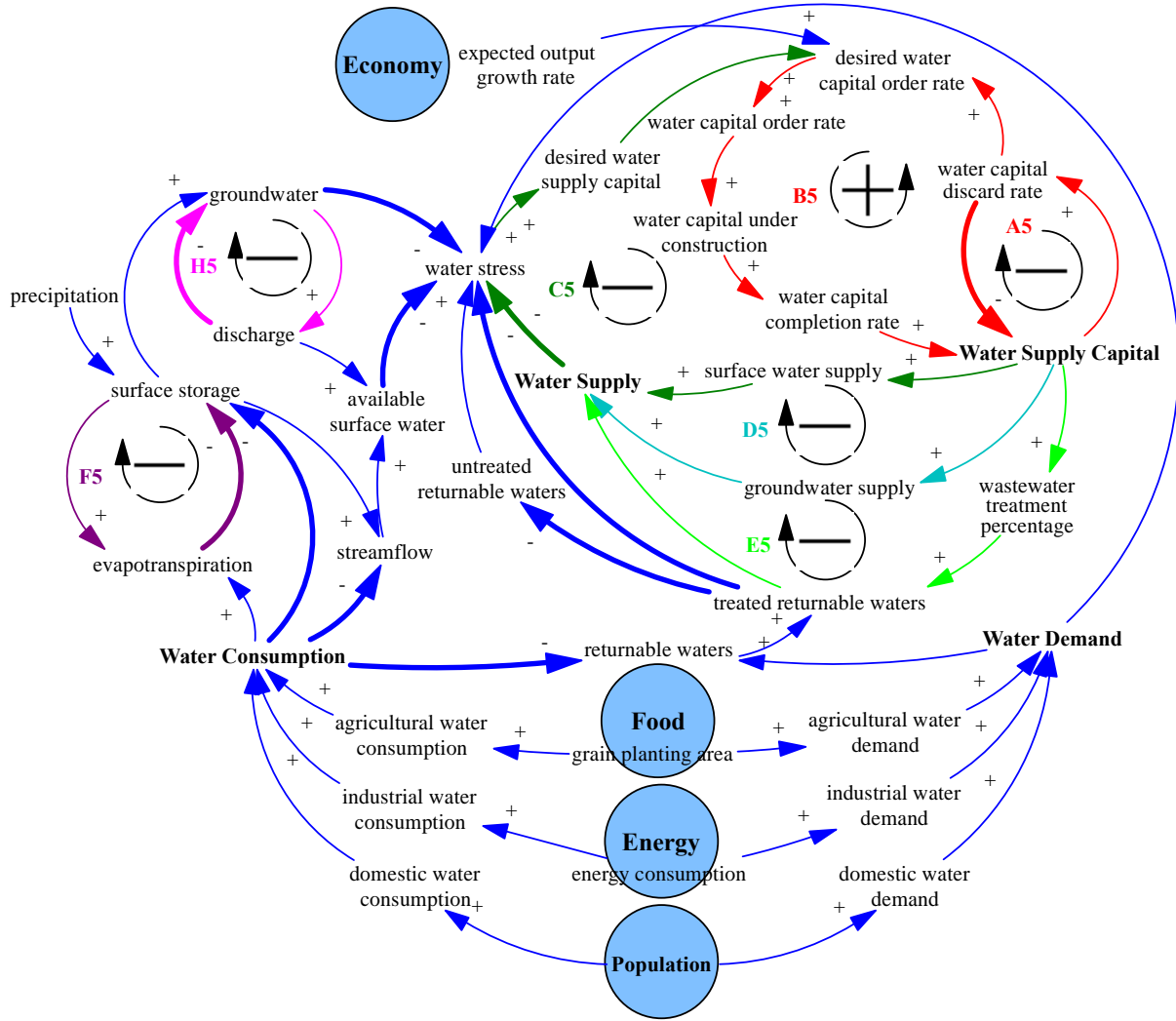


Figure 8 Causal feedback loops of the *Water Sector*

The modelling of the *base domestic water withdrawal* (structural water intensity) is based on the conceptual model presented in [Alcamo et al. \(2003\)](#), which was confirmed by the [IHP \(2000\)](#) data.

$$DSWI = DSWI_{min} + DSWI_{max}(1 - \exp(-\gamma_d GDP_{pcap}^{1.5})) \quad (29)$$

where  $DSWI$  = domestic structural water intensity ( $m^3/person$ ),  $GDP_{pcap}$  means GDP per capita.  $DSWI_{min}$ ,  $DSWI_{max}$ , and  $\gamma_d$  are calibrated parameters.

Using the domestic structural water intensity presented above, *domestic water demand* can be calculated as,



$$W_{dom} = DSWI \cdot P \cdot \Delta TFP \quad (30)$$

where  $W_{dom}$  = domestic water demand ( $10^8 \text{ m}^3/\text{year}$ ),  $P$  is the population (person),  $\Delta TFP$  is change in total factor productivity and represents changes in domestic water use efficiency.

The generation of electricity typically dominates water withdrawals in the industrial sector. In this model, the production of electricity consists of both nonrenewable sources (coal-fired and gas-fired thermal power) and renewable sources (hydropower and nuclear power).

The water withdrawal and water consumption of thermal power vary substantially among different cooling methods, and their values for different fuel source are obtained from [Zhang et al. \(2016\)](#) which is shown in **Table 6**.

Table 6 Water withdrawal and consumption factors for electricity production

Energy source	Cooling method	Water withdrawal factor ( $\text{m}^3/\text{MWh}$ )	Water consumption factor ( $\text{m}^3/\text{MWh}$ )
Coal	OT	98.54	0.393
	RC	2.466	1.972
	DRY	0.438	0.448
Gas	OT	34.07	0.379
	RC	2.902	2.114
Nuclear	OT (seawater)	178	1.514
Hydro		0	0

Note: Extracted from [Zhang et al. 2016](#). OT=once through, RC=recirculating

The nuclear power in the Yangtze river basin only withdrawals seawater, so the water withdrawal and consumption factors of Nuclear power are all set to zero with respect to fresh water.

$$W_{ele} = Tech_{ele} \cdot \sum_{i=1}^4 E_{P_i} \cdot \sum_{j=1}^n WWF_{i,j} \cdot F_{i,j} \quad (31)$$

where  $W_{ele}$  = electricity water demand ( $10^8 \text{ m}^3/\text{year}$ );  $E_{Pi}$  is electricity production for energy source  $i$  ( $10^8 \text{ kWh}$ );  $WWF_i$  is water withdrawal factor for energy source  $i$  ( $\text{m}^3/\text{MWh}$ );  $F_{i,j}$  is the fraction of cooling method  $j$  for energy source  $i$  (dml);  $Tech_{ele}$  is technological change for withdrawals in electricity production.

$$W_{ind} = \frac{1}{R_{ele}} \cdot W_{ele} \quad (32)$$

where  $W_{ind}$  = industrial water demand ( $10^8 \text{ m}^3/\text{year}$ );  $R_{ele}$  is the ratio of electricity water demand to industrial water demand.

*Agricultural water demand* is the production of per hectare agricultural water withdrawal and net arable land that is used to grow food.

$$W_{agr} = PHW \cdot A_l \quad (33)$$

where  $W_{agr}$  = agricultural water demand ( $10^8 \text{ m}^3/\text{year}$ );  $PHW$  = per hectare water withdrawal ( $\text{m}^3/\text{hectare}/\text{year}$ );  $A_l$  = net arable land (hectare).

Agricultural water usually decreases as irrigation efficiency increases along with technological progress. Changes in global surface temperature can also affect water demand for *food production* as increased temperatures lead to higher *evapotranspiration* rates in agricultural soils, thereby leaving less water for the crops and boosting irrigation water requirements (Yuan et al. 2016). Irrigation efficiency and *temperature feedback* are taken into account in *per hectare water withdrawal*, which is represented as,

$$PHW = BW_{agr} \cdot Tech_{agr} \cdot T_{feedback} \quad (34)$$

where  $BW_{agr}$  = base specific water withdrawal for agriculture ( $\text{m}^3/\text{hectare}/\text{year}$ );  $Tech_{agr}$  is technological change factor for irrigation;  $T_{feedback}$  is temperature feedback multiplier.

*Water stress* has four definitions. The *base water stress* is represented as,

$$WS_{base} = \frac{W_{dom}+W_{ind}+W_{agr}}{SW_{avai}} \quad (35)$$

where  $WS_{base}$  = base water stress,  $SW_{avai}$  = available surface water.

The *water stress with groundwater and wastewater* is represented as,

$$WS_{gw+ww} = \frac{W_{dom}+W_{ind}+W_{agr}}{SW_{avai}+r_{gw} \times GW+TRW} \quad (36)$$

where  $WS_{gw+ww}$  = water stress with groundwater and wastewater,  $r_{gw}$  = groundwater use ratio, which takes the value of 0.01 in this study,  $GW$ = groundwater,  $TRW$  = treated returnable waters.

The *water stress with pollution effects* is represented as,

$$WS_{pollution} = \frac{W_{dom}+W_{ind}+W_{agr}}{SW_{avai}-f_{ww} \times UTRW} \quad (37)$$

where  $WS_{pollution}$  = water stress with pollution effects,  $f_{ww}$  = wastewater pollution factor, which takes the value of 8 in this study,  $UTRW$  = untreated returnable waters.

The *water stress with water supply capacity* is represented as,

$$WS_{supply} = \frac{W_{dom}+W_{ind}+W_{agr}}{TWS} \quad (38)$$

where  $WS_{supply}$  = water stress with water supply capacity,  $TWS$  = total water supply capacity, which is the sum of surface water supply capacity, groundwater supply capacity, and treated returnable waters.

Some of the major parameters and initial values in the *Water Sector* are provided in **Table 7**.

Table 7 Major parameters and their corresponding values in the *Water Sector*

Variable	Value	Unit	Note
initial surface water	11890	10 <sup>8</sup> m <sup>3</sup>	
initial groundwater	594488	10 <sup>8</sup> m <sup>3</sup>	
initial domestic wastewater treatment percentage	30	percent	
initial industrial wastewater treatment percentage	40	percent	
stable and useable runoff percentage	37	percent	From ANEMI
groundwater use ratio	0.01	dmnl	
wastewater pollution factor	8	dmnl	From ANEMI

### 3.7 Carbon Sector

The carbon cycle in ANEMI\_Yangtze is based on the carbon cycle of ANEMI, which has its origin in [Goudriaan and Ketner \(1984\)](#). As this research is at a regional scale, the carbon cycles in the ocean and the atmosphere are excluded. Only the carbon cycle at a terrestrial scale is considered. The total carbon emissions into the air consist of the fossil fuel carbon emissions from the *Energy Sector* and the land-use carbon emissions from the *Land Sector*.

The causal loop diagram of the *Carbon Sector* is given in **Figure 9**. The chain of negative feedback loops passing through each of the terrestrial carbon stocks from the *biomass* to *litter*, to *humus*, and to *stable humus and charcoal* (A6, B6, C6) and the negative feedback loops depicting the decaying (E6, G6, H6, I6) and burning (D6, F6) process of each carbon stock all act as a positive feedback loop in the atmosphere-terrestrial carbon cycle (K6 and J6). An increase in atmospheric carbon results in higher uptake of carbon in the *biomass* through the effect of *net primary productivity*, which results in greater transfer of carbon through the chain (*biomass, litter, humus, stabilized humus and charcoal*) thereby leading to an increase in decay and transfer of carbon back to the atmosphere.

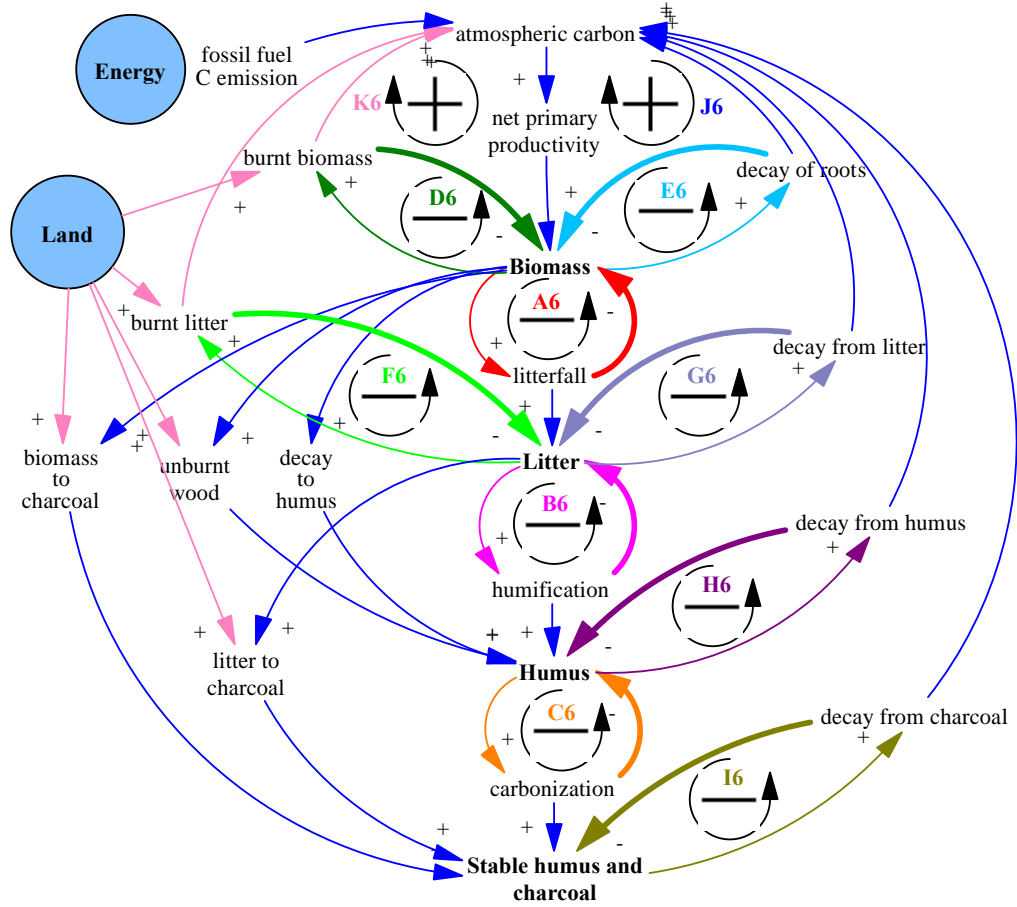


Figure 9 Causal feedback loops of the *Carbon Sector*

The accumulation of carbon in the atmosphere can be expressed as,

$$C_A = \int (D_B + D_L + D_H + D_K - NPP + B_B + B_L + E_{ind}) dt \quad (39)$$

where  $C_A$  = atmospheric carbon (Tg C/year),  $D_B$  = decay of biomass (Tg C/year),  $D_L$  = decay of litter (Tg C/year),  $D_H$  = decay of humus (Tg C/year),  $D_K$  = decay of charcoal (Tg C/year),  $NPP$  = net primary productivity (Tg C/year),  $B_B$  = burning of biomass (Tg C/year),  $B_L$  = burning of litter (Tg C/year),  $E_{ind}$  = industrial emissions (Tg C/year).

*Net primary productivity* is calculated as,

$$NPP_{jk} = p_{jk} \cdot \sigma(NPP_j) \cdot \frac{A_j}{10^{12}} \quad (40)$$

where  $j$  = biome type (agricultural land, forest, grassland, wetland, settlement, other land),  $k$  = biomass component (leaf, branch, stem, root),  $p_{jk}$  = fraction of biomass partitioned to component  $k$  of biome  $j$ ,  $\sigma(NPP_j)$  = variable surface density of net primary production (g C/m<sup>2</sup>/year),  $A_j$  = biome area (m<sup>2</sup>).

The variable surface density of net primary production is represented as,

$$\sigma(NPP_j) = \sigma(NPP_j)_0 \cdot \left(1 + \beta \cdot \ln\left(\frac{C_A}{C_{A0}}\right)\right) \quad (41)$$

where  $\sigma(NPP_j)_0$  = base surface density (g C/m<sup>2</sup>/year),  $\beta$  = CO<sub>2</sub> fertilization factor,  $C_A$  = current atmospheric CO<sub>2</sub>,  $C_{A0}$  = initial atmospheric CO<sub>2</sub>.

The amount of carbon stored in each component  $k$  of the *biomass* stock for each biome type  $j$  is represented as,

$$B_{jk} = \int \left( NPP_{jk} - FL_{B_{jk}} - FH_{B_{jk}} - FR_{B_{jk}} - B_{B_{jk}} - BK_{B_{jk}} - UB_{B_{jk}} \right) dt \quad (42)$$

where  $FL_{B_{jk}}$  = amount of litter falling from biomass to litter layer,  $FH_{B_{jk}}$  = decay of biomass to humus,  $FR_{B_{jk}}$  = decay of roots,  $B_{B_{jk}}$  = burning of biomass,  $BK_{B_{jk}}$  = burning of biomass to charcoal,  $UB_{B_{jk}}$  = unburned remainder of biomass.

Carbon accumulated in the *litter* stock is represented as,

$$L_j = \int \left( \sum_{k=1}^4 FL_{B_{jk}} - D_{L_j} - FH_{L_j} - B_{L_j} - FL_{K_j} \right) dt \quad (43)$$

where  $\sum_{k=1}^4 FL_{B_{jk}}$  = total litterfall,  $D_{L_j}$  = decay of carbon from litter to atmosphere,  $FH_{L_j}$  = decomposition of litter into humus,  $B_{L_j}$  = burning of carbon from litter to atmosphere,  $FL_{K_j}$  = burning of carbon from litter directly to charcoal.

The *humus* carbon stock is calculated as,

$$H_j = \int \left( \sum_{k=1}^4 FB_{B_{jk}} + FH_{L_j} - FK_{H_j} - D_{H_j} + \sum_{k=1}^4 UB_{jk} + FH_{H_j} \right) dt \quad (44)$$

where  $\sum_{k=1}^4 FB_{B_{jk}}$  = decay of biomass to humus,  $FH_{L_j}$  = decomposition of litter into humus,  $FK_{H_j}$  = decomposition of humus to charcoal,  $D_{H_j}$  = decay of humus to the atmosphere,  $\sum_{k=1}^4 UB_{jk}$  = unburnt remainder of biomass,  $FH_{H_j}$  = internal flow of humus.

The *stable humus and charcoal* carbon stock can be expressed as,

$$K_j = \int \left( FK_{H_j} - D_{K_j} + \sum_{k=1}^4 FK_{B_{jk}} + FK_{L_j} - FK_{K_j} \right) dt \quad (45)$$

where  $FK_{H_j}$  = flow of carbon from humus to charcoal,  $D_{K_j}$  = decay of charcoal,  $\sum_{k=1}^4 FK_{B_{jk}}$  = burning of biomass directly into charcoal,  $FK_{L_j}$  = carbon flow from litter to charcoal,  $FK_{K_j}$  = internal flow of charcoal from one biome to another.

Some of the major parameters and the initial values in the *Carbon Sector* are provided in **Tables 8-10**.

Table 8 Major parameters and their corresponding values in the *Carbon Sector*

Variable	Value	Unit	Note
coal emission factor	0.7559	t C/ t coal	
oil emission factor	0.5857	t C/t oil	
gas emission factor	0.4483	t C/t gas	

Table 9 Initial carbon stock and base surface density of NPP values

Biome	leaf (Tg)	branch (Tg)	stem (Tg)	root (Tg)	litter (Tg)	humus (Tg)	charcoal (Tg)	base surface density of NPP (g C/m <sup>2</sup> /year)
Agricultural land	1509	0	0	377	845	4853	4853	500
Forest	103	769	3483	769	623	3366	8479	900
Grassland	23.53	0	0	16.34	78.9	1582	975	195
Wetland	3.1	1.5	3.1	7.7	23.1	133	133	430
Settlement	1.5	7.2	56.2	7.2	5.1	62	62	100
Other land	2	3.8	19.2	2.3	10.8	236	149	70

Table 10 Parameters of the flow through the terrestrial biosphere

Item	agriculture	forest	grassland	wetland	settlement	other
partitioning ( $p_{jk}$ )						
leaf	0.8	0.3	0.6	0.3	0.3	0.5
branch	0	0.2	0	0.2	0.2	0.1
stem	0	0.3	0	0.2	0.3	0.1
root	0.2	0.2	0.4	0.3	0.2	0.3
life span ( $\tau$ )						
leaf	1	1	1	1	1	1
branch	10	10	10	10	10	10
stem	50	30	50	30	50	50
root	1	10	1	10	10	2
litter	1	1	2	1	2	2
humus	25	10	40	10	50	50
charcoal	500	500	500	500	500	500
humification factor ( $\lambda$ )	0.2	0.4	0.6	0.4	0.5	0.6



carbonization factor ( $\phi$ ) upon decomposition	0.05	0.05	0.05	0.05	0.05	0.05
carbonization factor ( $\epsilon_k$ ) on burning of leaf is 0.05, of branch 0.1, of stem 0.2, and of litter ( $\epsilon_L$ ) is 0.1.						

### 3.8 Nutrients Sector

In ANEMI\_Yangtze, nutrients (nitrogen, phosphorus) concentration in surface waters is used to indicate water pollution. Wastewater from domestic and industrial users and agricultural inputs are the main contributors to water quality degradation. The index of water pollution is a multiplier on life expectancy in the *Population Sector*.

The causal loop diagram of the *Nutrients Sector* is given in **Figure 10**. The cycles of phosphorous and nitrogen basically follow that of the carbon cycle. Take phosphorous cycle, for example, the chain of negative feedback loops passing through *land biota* to *humus* and to *rivers* (A7, B7, C7, D7, E7) and the negative feedback loops depicting the *weathering of inorganic P* (F7) act as a positive feedback loop in the terrestrial phosphorous cycle (H7). Because it represents a continuous cycle of negative feedbacks, it will attempt to reach equilibrium under natural conditions. Anthropogenic influences on this system in the form of wastewater discharge affect this equilibrium and drive change in the nutrient cycles.

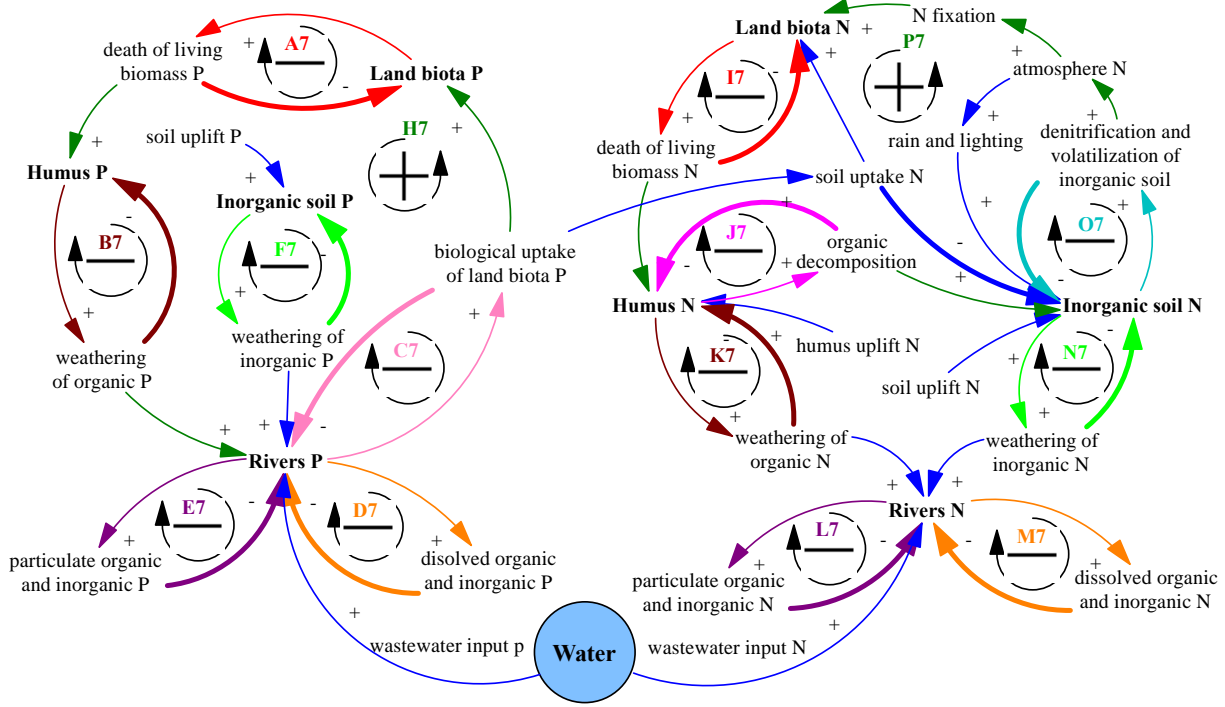


Figure 10 Causal feedback loops of the *Nutrients Sector*

Each flow in the nutrients cycle model is represented as negative feedback with a first-order material delay and an implicit goal of zero. The mathematical representation of the nutrients cycle takes the following structure,

$$N_i = \int (k_{ijN} \cdot N_j + F_{ijN}) dt \quad [nN] \quad (46)$$

$$P_i = \int (k_{ijP} \cdot P_j + F_{ijP}) dt \quad [nP] \quad (47)$$

where  $i$  = index for originating nutrient reservoir,  $j$  = index for receiving nutrient reservoir,  $k_{ijN}$  = rate constant matrix for  $N$  flows from nutrient reservoir  $i$  to  $j$ ,  $k_{ijP}$  = rate constant matrix for  $P$  flows from nutrient reservoir  $i$  to  $j$ ,  $N_i$  = nitrogen reservoir  $i$ ,  $P_i$  = phosphorus reservoir  $i$ ,  $F_{ijN}$  = constant nitrogen flow from reservoir  $i$  to  $j$ ,  $F_{ijP}$  = constant phosphorus flow from reservoir  $i$  to  $j$ .

The inputs of  $N$  and  $P$  in the nutrients cycle are calculated from the wastewaters in the domestic and industrial sectors as well as from agricultural returnable flows. For domestic and industrial wastewaters, the nutrients inputs are calculated based on the amount of untreated wastewater

adjusted for wastewater reuse and treated wastewater with exogenous removal efficiencies of  $N$  and  $P$  applied.

$$NE_{N_{dom}} = (DW_{untreated} - W_{ww_{dom}} + DW_{treated} \cdot (1 - N_{removal_{eff}})) \cdot N_{conc_{dom}} \quad (48)$$

$$NE_{P_{dom}} = (DW_{untreated} - W_{ww_{dom}} + DW_{treated} \cdot (1 - P_{removal_{eff}})) \cdot P_{conc_{dom}} \quad (49)$$

$$NE_{N_{ind}} = (IW_{untreated} - W_{ww_{ind}} + IW_{treated} \cdot (1 - N_{removal_{eff}})) \cdot N_{conc_{ind}} \quad (50)$$

$$NE_{P_{ind}} = (IW_{untreated} - W_{ww_{ind}} + IW_{treated} \cdot (1 - P_{removal_{eff}})) \cdot P_{conc_{ind}} \quad (51)$$

where  $NE$  = nutrients emission (nN/year for nitrogen and nP/year for phosphorus),  $DW$  = domestic wastewater,  $IW$  = industrial wastewater,  $W_{ww}$  = wastewater reuse,  $N_{removal_{eff}}$  = exogenous  $N$  removal efficiency,  $P_{removal_{eff}}$  = exogenous  $P$  removal efficiency,  $N_{conc}$  = concentration of  $N$  in wastewater,  $P_{conc}$  = concentration of  $P$  in wastewater.

Agricultural nutrients inputs are based on the amount of *arable land* that is used for food production and the nutrients leaching factors.

$$NE_{N_{agr}} = A_l \cdot N_{leaching} \quad (52)$$

$$NE_{P_{agr}} = A_l \cdot P_{leaching} \quad (53)$$

where  $A_l$  = net arable land,  $N_{leaching}$  = leaching factor for  $N$  from net arable land,  $P_{leaching}$  = leaching factor for  $P$  from net arable land.

The inputs of nutrients to surface waters in the nutrients cycle is based on the excess amount from the initial nutrients inputs because of the assumption that the nutrients cycle is assumed to start at a quasi-steady state solution.

Some of the major parameters in the *Nutrients Sector* are given in **Table 11**.

Table 11 Major parameters and their corresponding values in the *Nutrients Sector*

Variable	Value	Unit	Note
N concentration of domestic wastewater	60	g/L	Henze and Comeau (2008)
N concentration of industrial wastewater	60	g/L	
P concentration of domestic wastewater	15	g/L	
P concentration of industrial wastewater	15	g/L	
N leaching coefficient of agricultural runoff	18.65	kg/ha/year	FAO (2019)
P leaching coefficient of agricultural runoff	0.415	kg/ha/year	FAO (2019)

The initial values and rate constants in the model are abstracted from ANEMI by multiplying a scale factor *global to Yangtze scaling factor*, which equals the ratio of Yangtze population to the global population of China in 1990.

### 3.9 Fish Sector

The *Fish Sector*, which is an entirely new addition to the ANEMI\_Yangtze model, is used to describe the dynamic of *fish biomass stock* and *fish yield* over time. There are four feedback loops that drive the dynamics of *fish biomass stock* (see **Figure 11**). Loops A8, C8, and D8 represent negative feedback on *fish biomass stock* through *natural fish death*, *fish recruits*, and *fish yield*, respectively. The wastewater water discharged from the *Water Sector* acts as a positive factor on *natural mortality*. Loop B8, which connects *total reservoir capacity* and *ship cargo volume* with *fish birth rate*, acts as positive feedback on *fish biomass stock*. As the *total reservoir capacity* and *ship cargo volume* increase, the *fish birth rate* decreases so too does the *fish birth*. The decline in *fish birth* decreases the *fish biomass stock*, which further reduces the *fish birth*.

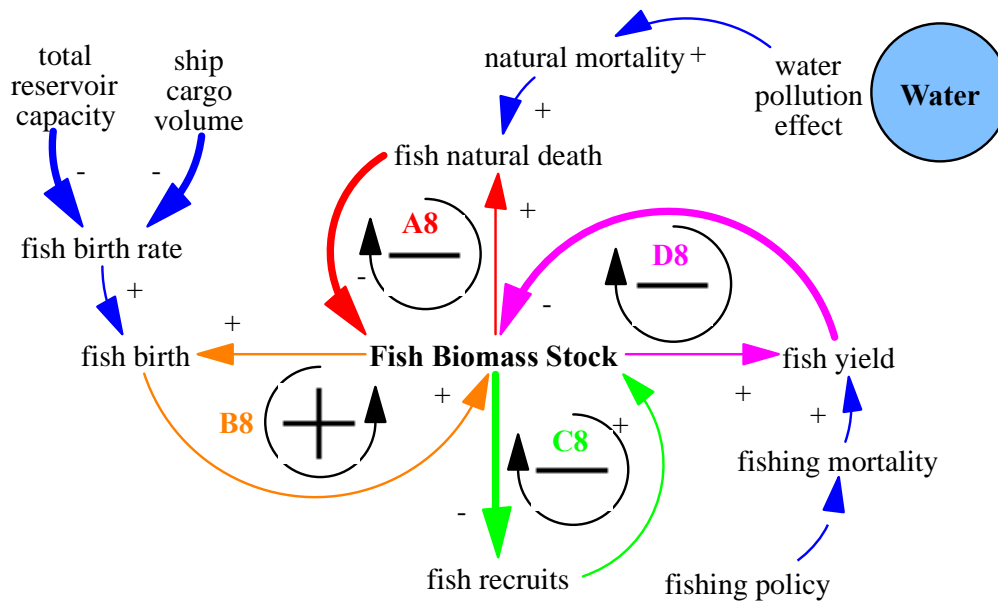


Figure 11 Causal feedback loops of the *Fish Sector*

The calculation of *fish biomass stock* is given as,

$$F = \int (f_b + f_r - f_d - f_y) dt \quad (54)$$

where  $F$  = fish biomass stock,  $f_b$  = fish birth,  $f_r$  = fish recruits, which is treated as an exogenous variable,  $f_d$  = natural fish death,  $f_y$  = fish yield.

Some of the major parameters and initial values in the *Fish Sector* are given in **Table 12**.

Table 12 Major parameters and their corresponding values in the *Fish Sector*

Variable	Value	Unit	Note
reference natural mortality	0.075	dmnl	<a href="#">Gilbert et al. (2000)</a>
reference fishing mortality	0.7949	dmnl	<a href="#">Chen et al. (2009)</a>
reference fish birth rate	0.826	dmnl	<a href="#">Zhang et al. (2020)</a>
Initial fish biomass stock	historical fish yield in 1990 / reference fishing mortality	tonne	

The value 0.7949 of reference fishing mortality is calculated based on [Chen et al. \(2009\)](#) by averaging the exploitation coefficients of 10 economically fish species (fishing mortality = 0.761, 0.706, 0.803, 0.829, 0.898, 0.876, 0.846, 0.774, 0.765 and 0.691). The value 0.826 of reference fish birth rate is calculated based on [Zhang et al. \(2020\)](#) by averaging fish growth rate in the middle reach, Dongting lake, and Poyang lake values.

## 4. MODEL VALIDATION AND SENSITIVITY ANALYSIS

The ANEMI\_Yangtze model was calibrated and validated sector by sector before putting all sectors together. In this section, we conducted the validation and sensitivity analysis of the model as a whole, *i.e.*, all of the cross-sectoral feedbacks are activated.

### 4.1 Model Validation

To verify the feasibility of ANEMI\_Yangtze, simulation results for the major state variables were compared to available historical data for 1990-2015. The results are shown in **Figure 12**.

As shown in **Figure 12**, the model can reproduce the system behaviours very well for *population*, *gross output*, and *water demand* (**Figures 12(a, b, and f)**). The model can capture the general system behaviour patterns for *energy requirement*, *energy production*, and *food production* (**Figures 12(c-e)**). The fluctuations of *food production* in the historical data are mainly attributed to the flood and drought disasters, which are not currently included in the model. The discrepancies between historical and simulated *energy requirement* and *energy production* are partly due to the past energy policies acting on the energy system that the ANEMI\_Yangtze model doesn't consider. All in all, with only a small number of exogenous inputs (mainly *precipitation* and *temperature* in *Water Sector*), this comprehensive feedback-based integrated modelling system demonstrates its superiority by producing a very close agreement with the real-world data.

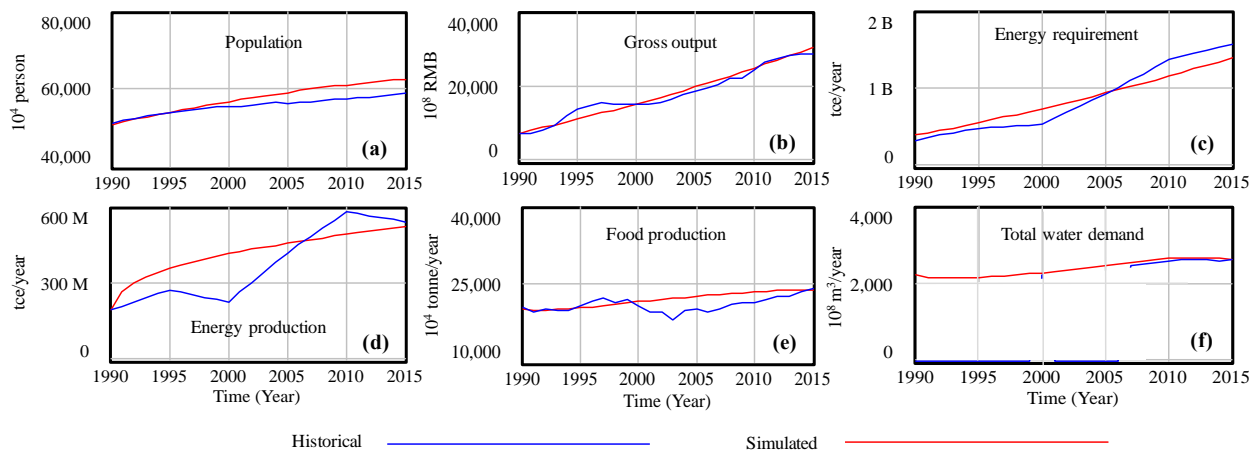


Figure 12 Comparison of simulated and historical system behaviours

## 4.2 Sensitivity Analysis

To test the sensitivity of ANEMI\_Yangtze, a set of variables are selected due to uncertainty in their values or the model structure for which they are used. The parameters used for the sensitivity test are shown in **Table 13**. To determine whether alternate types of system behaviour are possible by varying the baseline values of each selected parameter by -10 ~ 10%. Triangular probability distributions are used. The highest point of probability in the triangle is assigned to the baseline value of these parameters, where the outer limits are defined by the minimum and maximum percentage changes to the baseline value.

Table 13 Parameters used for the sensitivity test of key state variables in the model

State variable	Parameters	Baseline value
Yangtze population	life expectancy normal [upper, middle, lower]	50, 50, 55
	female ratio	0.5
	reproductive lifetime	35
Yangtze gross output	value share of labour [upper, middle, lower]	0.6, 0.62, 0.55
	capital energy substitution elasticity	0.75
	capital lifetime	40
Yangtze food production	per capita food consumption	400
	average life of land normal	6000
	inherent land fertility [upper, middle, lower]	4500, 6300, 6600
Yangtze energy production	energy resource elasticity [coal, oil, gas, hydro, nuclear, new]	0.625, 0.657, 0.657, 0.303, 0.303, 0.527
	energy capital lifetime [coal, oil, gas, hydro, nuclear, new]	15, 15, 15, 30, 30, 20
	ref energy consumption per unit GDP	6
Yangtze water demand	ref water withdrawal factor [coalOT, coalRC, coalDRY, gasOT, gasRC, hydroNO, nuclearOT]	98.54, 2.47, 0.44, 34.07, 2.90, 0, 0
	initial water intake [upper, middle, lower]	2100, 4000, 4500
Nitrogen concentration	N leaching coefficient of agricultural runoff	18.65
	N concentration domestic wastewater	60
	N concentration industrial wastewater	60

The sensitivity simulations are first performed separately for each state variable using their associated parameters only. The results for each of the variables examined in **Figure 13**, are shown as ranges for each confidence level. The 100% confidence level includes the range for a given



variable, including all outputs for the Monte Carlo simulations. As the confidence level decreases, the range of the projected variables becomes smaller. As can be seen from **Figure 13**, for each of the variables examined, the behaviour modes are the same within the range of the parameters tested, indicating the robustness of the model.

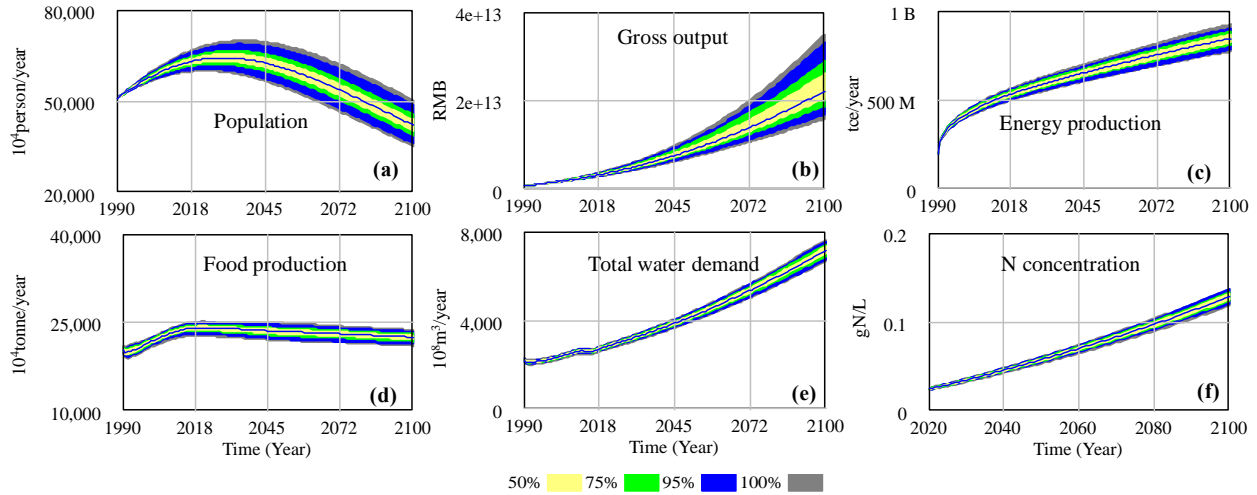


Figure 13 Sensitivity of selected state variables

The sensitivity simulations are then performed for all of the state variables listed in **Table 13**, considering all the possible parameter change combinations together. The results, seen in **Figure 14**, show that even the range in the trajectory of the state variables is larger compared to the results in Figure 13, the behaviour of each variable still remains the same, signifying the robustness of the model.

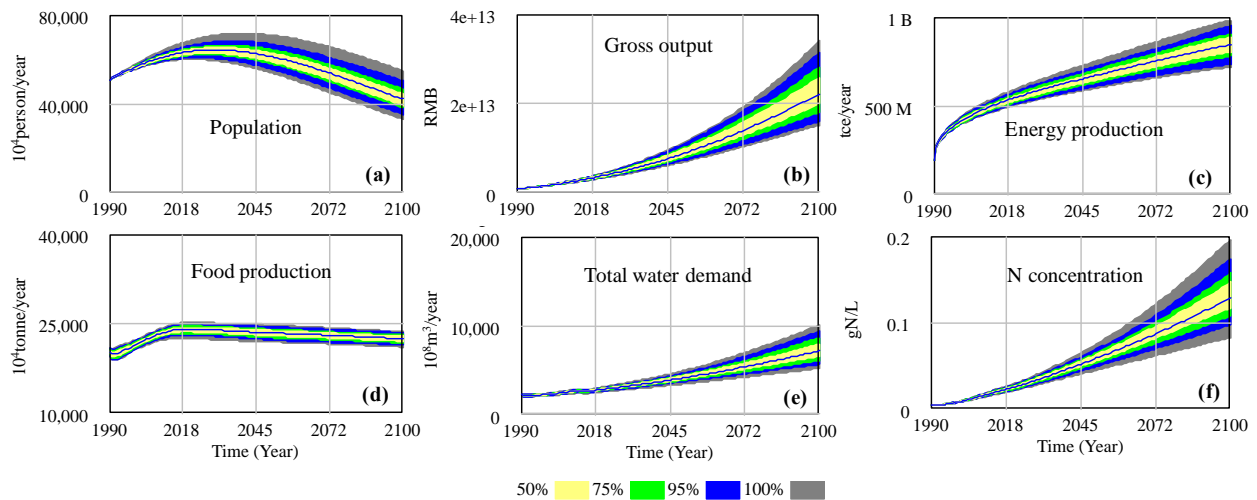


Figure 14 Total sensitivity of selected state variables

## **5. CLOSING REMARK**

The report provides a detailed introduction of the ANEMI\_Yangtze model developed at the University of Western Ontario. The focus of the report is on the model structure and its details with the presentation of the model validation results. We have conducted six experiments (S\_Climate, S\_Population, S\_Land use, S\_Energy, S\_Water, and S\_Eco-environment scenarios) using the ANEMI\_Yangtze model (details of the model results are to available in coming publications). S\_Climate scenario allows for the investigation of climate change impacts on social-economic development and natural resources in Yangtze river basin. S\_Population scenario provides an investigation of how changes in birth control policy affect population dynamics and the feedback between population growth and the depletion of natural resources and water pollution. S\_Land scenario allows for the investigation of the burning forest to expand agricultural land and to claim agricultural land for settlement and their combined impacts on population, economy, food, energy, carbon, and water systems. S\_Energy scenario allows for the investigation of shifting energy consumption patterns impacts on natural and environmental systems. S\_Water scenario allows for the investigation of impacts of water-saving techniques, and S\_Eco-environment scenario provides for the assessment of how policies aimed at improving eco-environment situation shall affect the Yangtze Economic Belt system.

## 6. REFERENCES

1. Akhtar, M.K., Wibe, J., Simonovic, S.P. and MacGee, J., 2013. Integrated assessment model of society-biosphere-climate-economy-energy system. *Environmental Modelling & Software*, 49, pp.1-21.
2. Albrecht, T.R., Crootof, A. and Scott, C.A., 2018. The Water-Energy-Food Nexus: A systematic review of methods for nexus assessment. *Environmental Research Letters*, 13(4), p.043002.
3. Alcamo J., Döll P., Henrichs T., et al. (2003) Development and testing of the WaterGAP 2 global model of water use and availability. *Hydrological Sciences Journal*, 48:317-337. doi: 10.1623/hysj.48.3.317.45290.
4. Bazilian, M., Rogner, H., Howells, M., Hermann, S., Arent, D., Gielen, D., Steduto, P., Mueller, A., Komor, P., Tol, R.S. and Yumkella, K.K., 2011. Considering the energy, water and food nexus: Towards an integrated modelling approach. *Energy policy*, 39(12), pp.7896-7906.
5. Breach, P., 2020. Water Supply Capacity Development in the Context of Global Change.
6. Cai, W., Fangyuan, T. (2020). Spatiotemporal characteristics and driving forces of construction land expansion in Yangtze River economic belt, China. *PloS one*, 15(1), e0227299.
7. Calvin, K., Patel, P., Clarke, L., Asrar, G., Bond-Lamberty, B., Cui, R.Y., Vittorio, A.D., Dorheim, K., Edmonds, J., Hartin, C. and Hejazi, M., 2019. GCAM v5. 1: representing the linkages between energy, water, land, climate, and economic systems. *Geoscientific Model Development*, 12(2), pp.677-698.
8. Chen, D., Xiong, F., Wang, K., & Chang, Y. (2009). Status of research on Yangtze fish biology and fisheries. *Environmental Biology of Fishes*, 85(4), 337-357.
9. Clayton, T. and Radcliffe, N., 2018. Sustainability: a systems approach. Routledge.
10. Daher, B.T. and Mohtar, R.H., 2015. Water–energy–food (WEF) Nexus Tool 2.0: guiding integrative resource planning and decision-making. *Water International*, 40(5-6), pp.748-771.
11. Davies, E.G., 2007. Modelling feedback in the Society-Biosphere-Climate system.
12. Davies, E.G. and Simonovic, S.P., 2010. ANEMI: a new model for integrated assessment of global change. *Interdisciplinary Environmental Review*, 11(2-3), pp.127-161.

13. D'Odorico, P., Davis, K.F., Rosa, L., Carr, J.A., Chiarelli, D., Dell'Angelo, J., Gephart, J., MacDonald, G.K., Seekell, D.A., Suweis, S. and Rulli, M.C., 2018. The global food - energy - water nexus. *Reviews of Geophysics*, 56(3), pp.456-531.
14. (FAO) Food and Agricultural Organization of the United Nations (2019) Eutrophication of Surface Waters. Fertilizers as Pollutants. <http://www.fao.org/3/w2598e/w2598e06.htm>. Accessed 15 Oct 2017.
15. Fiddaman T.S. (1997) Feedback Complexity in Integrated Climate-Economy Models. Ph.D. thesis. Department of Operations Management and System Dynamics, Massachusetts Institute of Technology, Cambridge, Massachusetts.
16. Flato, G., Marotzke, J., Abiodun, B., Braconnot, P., Chou, S.C., Collins, W., Cox, P., Driouech, F., Emori, S., Eyring, V. and Forest, C., 2014. Evaluation of climate models. In *Climate change 2013: the physical science basis. Contribution of Working Group I to the Fifth Assessment Report of the Intergovernmental Panel on Climate Change* (pp. 741-866). Cambridge University Press.
17. Garcia, D.J. and You, F., 2016. The water-energy-food nexus and process systems engineering: A new focus. *Computers & Chemical Engineering*, 91, pp.49-67.
18. Gilbert, D. J., McKenzie, J. R., Davies, N. M., & Field, K. D. (2000). Assessment of the SNA 1 stocks for the 1999–2000 fishing year. *New Zealand Fisheries Assessment Report*, 38, 52.
19. Goudriaan J. and P. Ketner (1984) A simulation study for the global carbon cycle, including man's impact on the biosphere. *Climatic Change* 6(2):167–192. doi: 10.1007/BF00144611.
20. Hamilton, S.H., ElSawah, S., Guillaume, J.H., Jakeman, A.J. and Pierce, S.A., 2015. Integrated assessment and modelling: overview and synthesis of salient dimensions. *Environmental Modelling & Software*, 64, pp.215-229.
21. Henze M. and Y. Comeau (2008) Wastewater Characterization. In: *Biological Wastewater Treatment: Principles Modelling and Design*. IWA Publishing, London, UK, pp 33-52.
22. Holman, I.P., Rounsevell, M.D.A., Cojocar, G., Shackley, S., McLachlan, C., Audsley, E., Berry, P.M., Fontaine, C., Harrison, P.A., Henriques, C. and Mokrech, M., 2008. The concepts and development of a participatory regional integrated assessment tool. *Climatic change*, 90(1), pp.5-30.

23. Hopwood, B., Mellor, M. and O'Brien, G., 2005. Sustainable development: mapping different approaches. *Sustainable development*, 13(1), pp.38-52.
24. IPCC (2001) Technical summary. *Climate change 2001: impacts, adaptation, and vulnerability. A Report of Working Group II of Intergovernmental Panel on Climate Change*. Cambridge University Press, New York.
25. Jakeman, A.J. and Letcher, R.A., 2003. Integrated assessment and modelling: features, principles and examples for catchment management. *Environmental Modelling & Software*, 18(6), pp.491-501.
26. Klein, J.T., Grossenbacher-Mansuy, W., Häberli, R., Bill, A., Scholz, R.W. and Welti, M. eds., 2001. *Transdisciplinarity: joint problem solving among science, technology, and society: an effective way for managing complexity*. Springer Science & Business Media.
27. Kling, C.L., Arritt, R.W., Calhoun, G. and Keiser, D.A., 2017. Integrated assessment models of the food, energy, and water nexus: A review and an outline of research needs. *Annual Review of Resource Economics*, 9, pp.143-163.
28. Li, J., Glibert, P.M., Zhou, M., Lu, S. and Lu, D., 2009. Relationships between nitrogen and phosphorus forms and ratios and the development of dinoflagellate blooms in the East China Sea. *Marine Ecology Progress Series*, 383, pp.11-26.
29. Li, Y., Acharya, K. and Yu, Z., 2011. Modeling impacts of Yangtze River water transfer on water ages in Lake Taihu, China. *Ecological Engineering*, 37(2), pp.325-334.
30. Liu, J., Dietz, T., Carpenter, S.R., Folke, C., Alberti, M., Redman, C.L., Schneider, S.H., Ostrom, E., Pell, A.N., Lubchenco, J. and Taylor, W.W., 2007. Coupled human and natural systems. *AMBIO: a journal of the human environment*, 36(8), pp.639-649.
31. Liu, Y., Wang, S. and Chen, B., 2017. Regional water-energy-food nexus in China based on multiregional input–output analysis. *Energy Procedia*, 142, pp.3108-3114.
32. Meadows D.H., Meadows D.L., Behrens W.W. and J. Randers (1972) *Limits to Growth*. Universe Books, New York.
33. Plevin, R.J., 2017. Assessing the climate effects of biofuels using integrated assessment models, part I: Methodological considerations. *Journal of Industrial Ecology*, 21(6), pp.1478-1487.
34. Prinn, R., Jacoby, H., Sokolov, A., Wang, C., Xiao, X., Yang, Z., Eckhaus, R., Stone, P., Ellerman, D., Melillo, J. and Fitzmaurice, J., 1999. *Integrated global system model for*

- climate policy assessment: Feedbacks and sensitivity studies. *Climatic change*, 41(3), pp.469-546.
35. Randall, D.A., Wood, R.A., Bony, S., Colman, R., Fichet, T., Fyfe, J., Kattsov, V., Pitman, A., Shukla, J., Srinivasan, J. and Stouffer, R.J., 2007. Climate models and their evaluation. In *Climate change 2007: The physical science basis. Contribution of Working Group I to the Fourth Assessment Report of the IPCC (FAR)* (pp. 589-662). Cambridge University Press.
  36. Rasul, G. and Sharma, B., 2016. The nexus approach to water-energy-food security: an option for adaptation to climate change. *Climate Policy*, 16(6), pp.682-702.
  37. Smajgl, A., Ward, J. and Pluschke, L., 2016. The water-food-energy Nexus - Realising a new paradigm. *Journal of Hydrology*, 533, pp.533-540.
  38. Sokolov, A.P., Schlosser, C.A., Dutkiewicz, S., Paltsev, S., Kicklighter, D.W., Jacoby, H.D., Prinn, R.G., Forest, C.E., Reilly, J.M., Wang, C. and Felzer, B.S., 2005. MIT integrated global system model (IGSM) version 2: model description and baseline evaluation. MIT Joint Program on the Science and Policy of Global Change.
  39. Stehfest E., van Vuuren D., Kram T., and L. Bouwman (2014) Overview of IMAGE 3.0. Integrated Assessment of Global Environmental Change with IMAGE 3.0: Model description and policy applications. PBL Netherlands Environmental Assessment Agency, pp 32–54.
  40. Stoy, P.C., Ahmed, S., Jarchow, M., Rashford, B., Swanson, D., Albeke, S., Bromley, G., Brookshire, E.N.J., Dixon, M.D., Haggerty, J. and Miller, P., 2018. Opportunities and trade-offs among BECCS and the food, water, energy, biodiversity, and social systems nexus at regional scales. *BioScience*, 68(2), pp.100-111.
  41. van Vuuren, D.P., Kok, M., Lucas, P.L., Prins, A.G., Alkemade, R., van den Berg, M., Bouwman, L., van der Esch, S., Jeuken, M., Kram, T. and Stehfest, E., 2015. Pathways to achieve a set of ambitious global sustainability objectives by 2050: explorations using the IMAGE integrated assessment model. *Technological Forecasting and Social Change*, 98, pp.303-323.
  42. Wang, H., Wang, G., Qi, J., Schandl, H., et al. (2020). Scarcity-weighted fossil fuel footprint of China at the provincial level. *Applied Energy*, 258, 114081.

43. Weitz, N., Strambo, C., Kemp-Benedict, E. and Nilsson, M., 2017. Closing the governance gaps in the water-energy-food nexus: Insights from integrative governance. *Global Environmental Change*, 45, pp.165-173.
44. Wong, C.M., Williams, C.E., Collier, U., Schelle, P. and Pittock, J., 2007. World's top 10 rivers at risk. *esocialsciences.com Working Papers*.
45. Xia, Y., Tabeta, S., Komatsuda, S. and Duan, F., 2016. The impacts of fishing and nutrient influx from Yangtze River on the ecosystem in East China Sea. *Modeling Earth Systems and Environment*, 2(3), pp.1-9.
46. Xu, H., Paerl, H.W., Qin, B., Zhu, G. and Gao, G., 2010. Nitrogen and phosphorus inputs control phytoplankton growth in eutrophic Lake Taihu, China. *Limnology and Oceanography*, 55(1), pp.420-432.
47. Xu, Z., Chen, X., Liu, J., Zhang, Y., Chau, S., Bhattarai, N., Wang, Y., Li, Y., Connor, T. and Li, Y., 2020. Impacts of irrigated agriculture on food–energy–water–CO<sub>2</sub> nexus across metacoupled systems. *Nature communications*, 11(1), pp.1-12.
48. Yang, S., Xu, K., Milliman, J. Yang, H. and Wu, C., 2015. Decline of Yangtze River water and sediment discharge: Impact from natural and anthropogenic changes. *Scientific Reports* 5, 12581. <https://doi.org/10.1038/srep12581>.
49. Yu, Z., Gu, H., Wang, J., Xia, J. and Lu, B., 2018. Effect of projected climate change on the hydrological regime of the Yangtze River Basin, China. *Stochastic environmental research and risk assessment*, 32(1), pp.1-16.
50. Zhang, C., Zhong, L., Fu, X., Wang, J., & Wu, Z. (2016). Revealing water stress by the thermal power industry in China based on a high spatial resolution water withdrawal and consumption inventory. *Environmental Science & Technology*, 50(4), 1642-1652.
51. Zhang, H., Kang, M., Shen, L., Wu, J., Li, J., Du, H., Wang, C., Yang, H., Zhou, Q., Liu, Z. and Gorfine, H., 2020. Rapid change in Yangtze fisheries and its implications for global freshwater ecosystem management. *Fish and Fisheries*, 21(3), pp.601-620.
52. Zhang, X. and Vesselinov, V.V., 2017. Integrated modeling approach for optimal management of water, energy and food security nexus. *Advances in Water Resources*, 101, pp.1-10.

## Appendix A: STOCK AND FLOW DIAGRAM OF EACH SECTOR

The stock and flow diagrams for each of the 9 sectors are provided in **Figures A1-A9**.

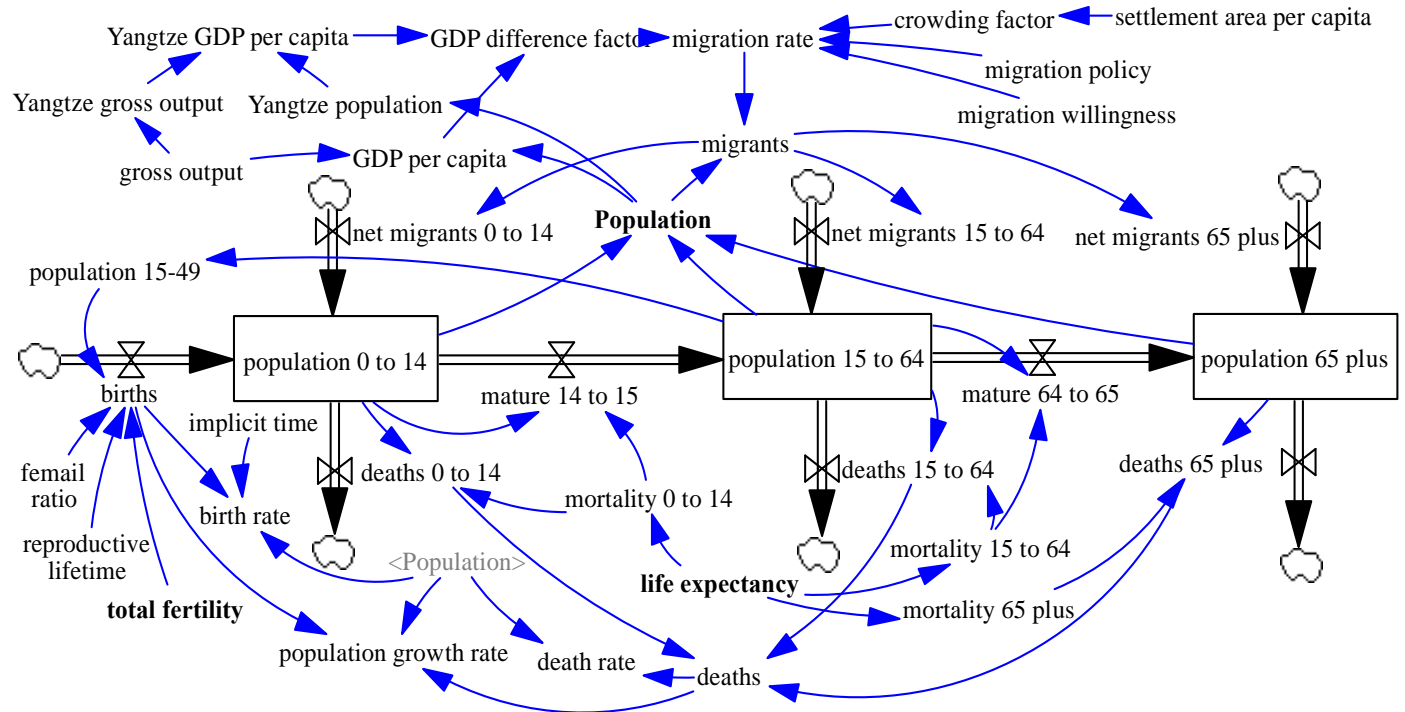


Figure A1 Stock and flow diagram of the *Population Sector*



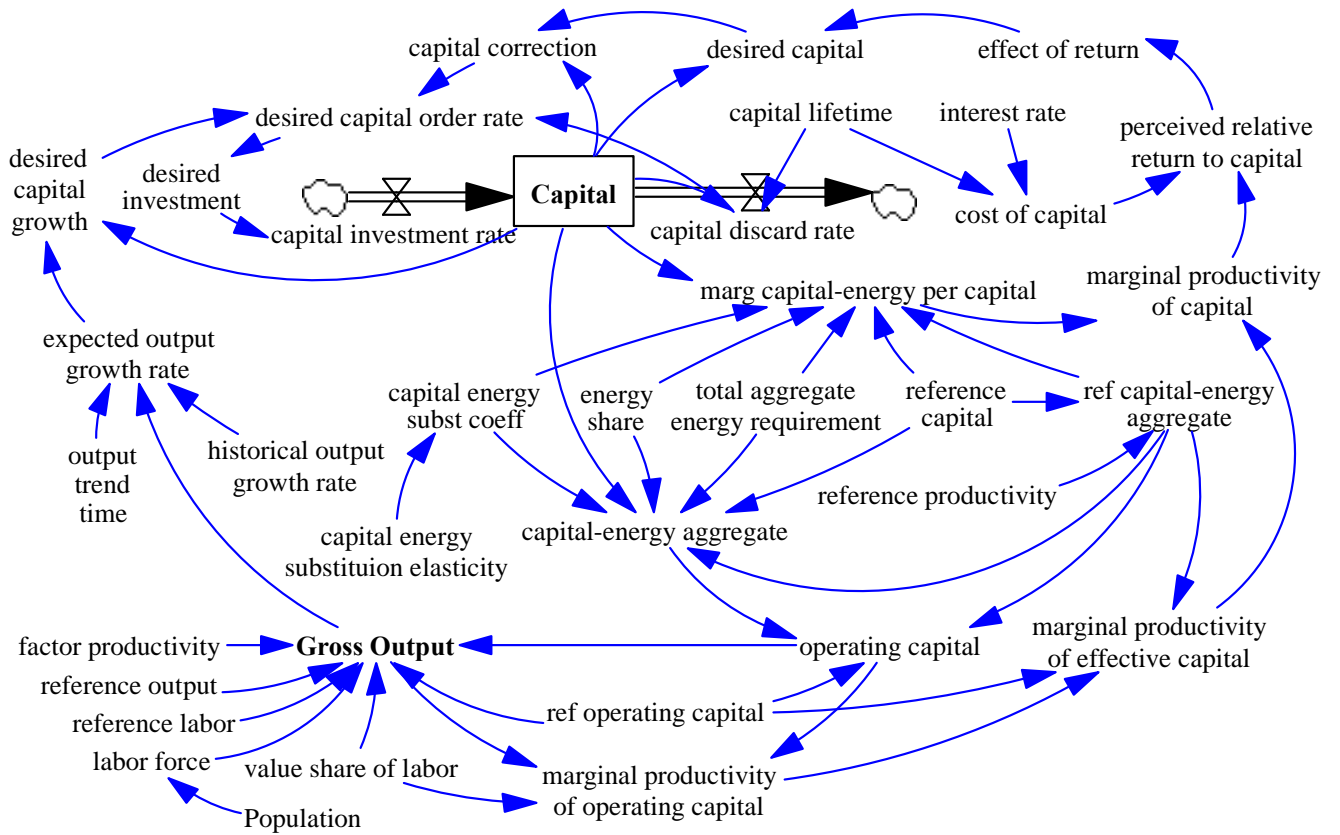


Figure A2 Stock and flow diagram of the *Economy Sector*

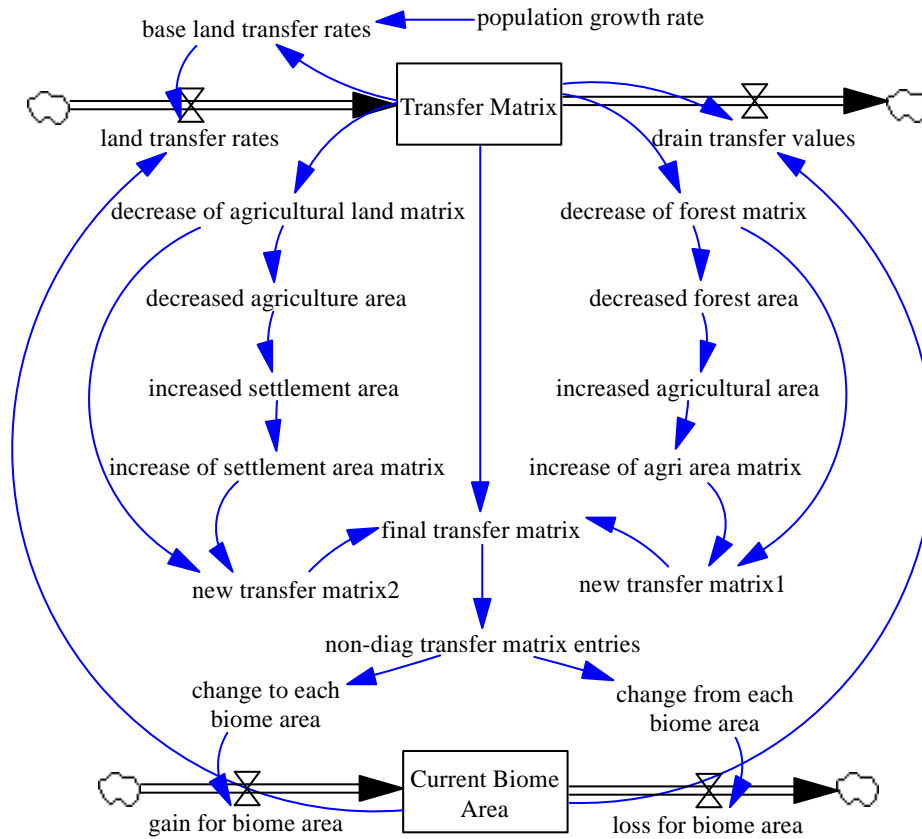


Figure A3 Stock and flow diagram of the *Land Sector*

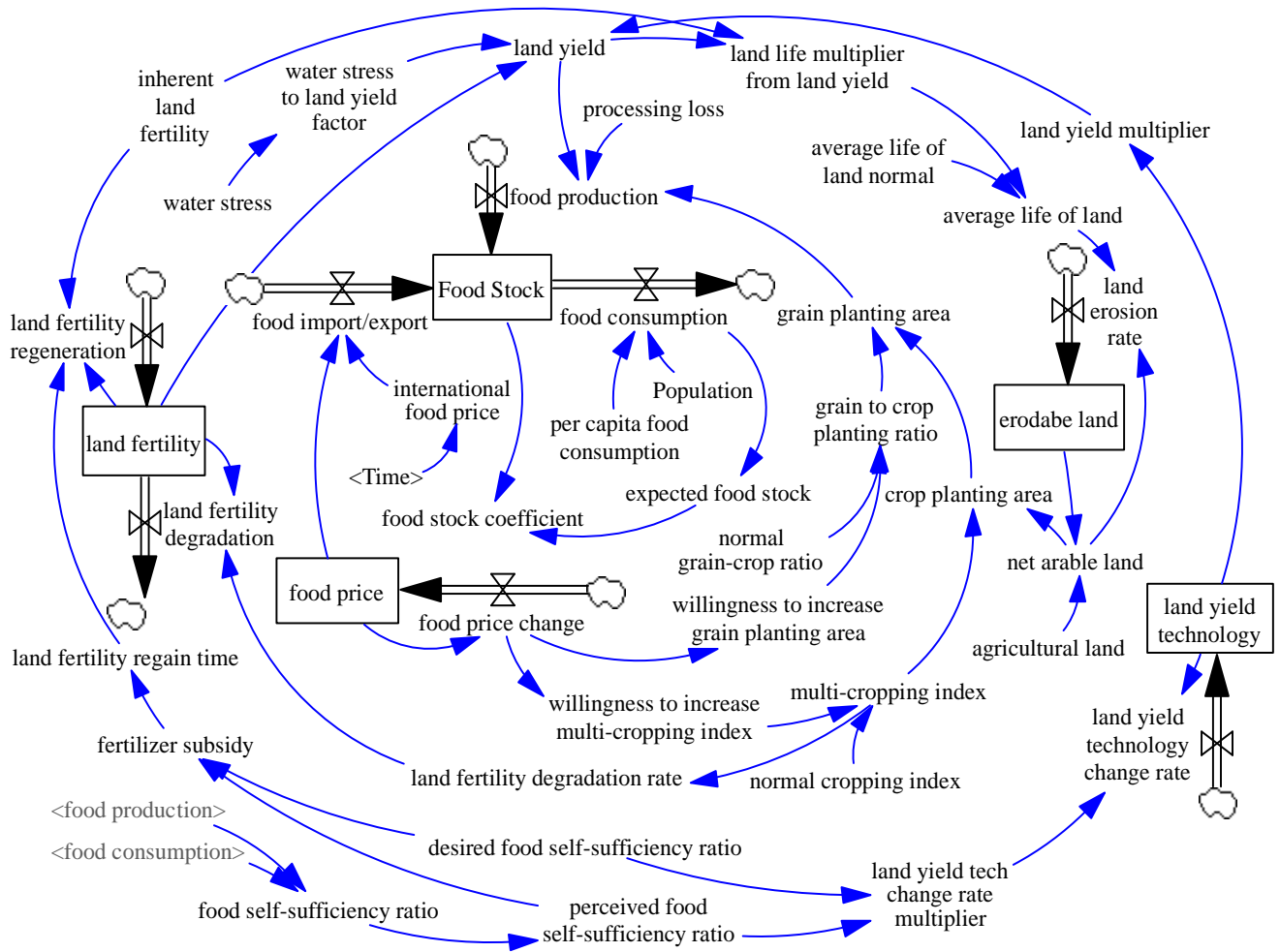


Figure A4 Stock and flow diagram of the *Food Sector*

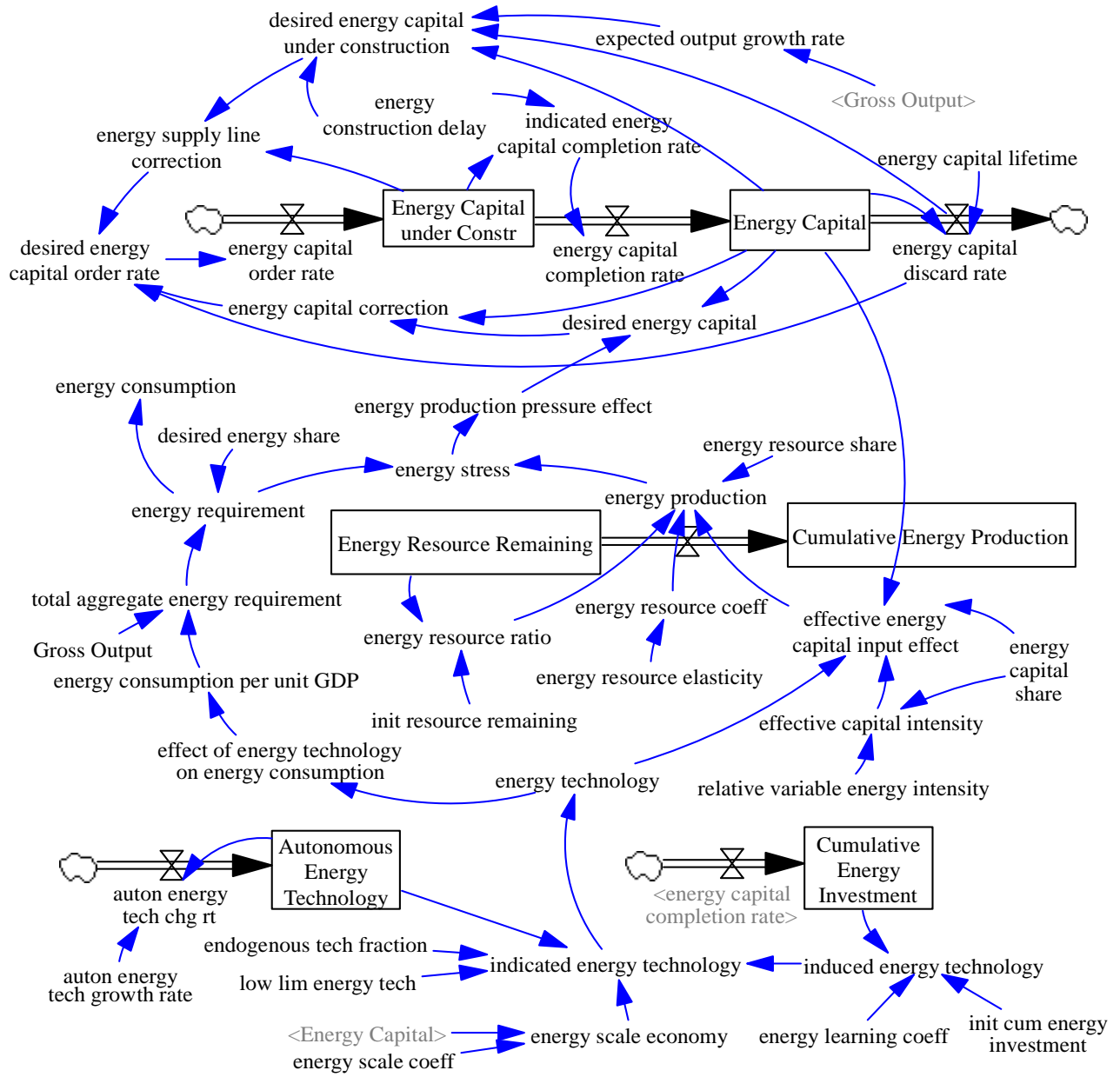


Figure A5 Stock and flow diagram of the *Energy Sector*

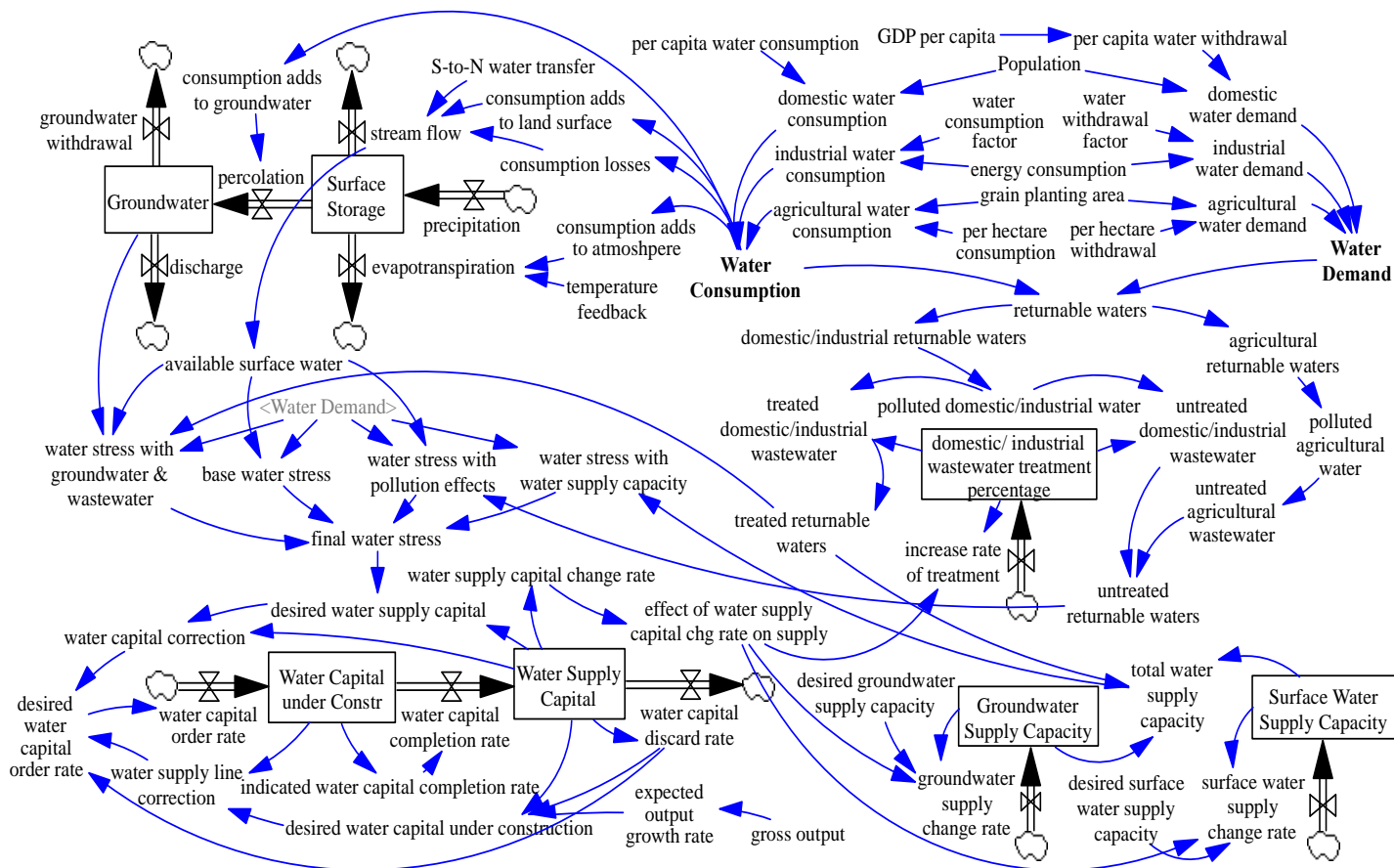


Figure A6 Stock and flow diagram of the *Water Sector*

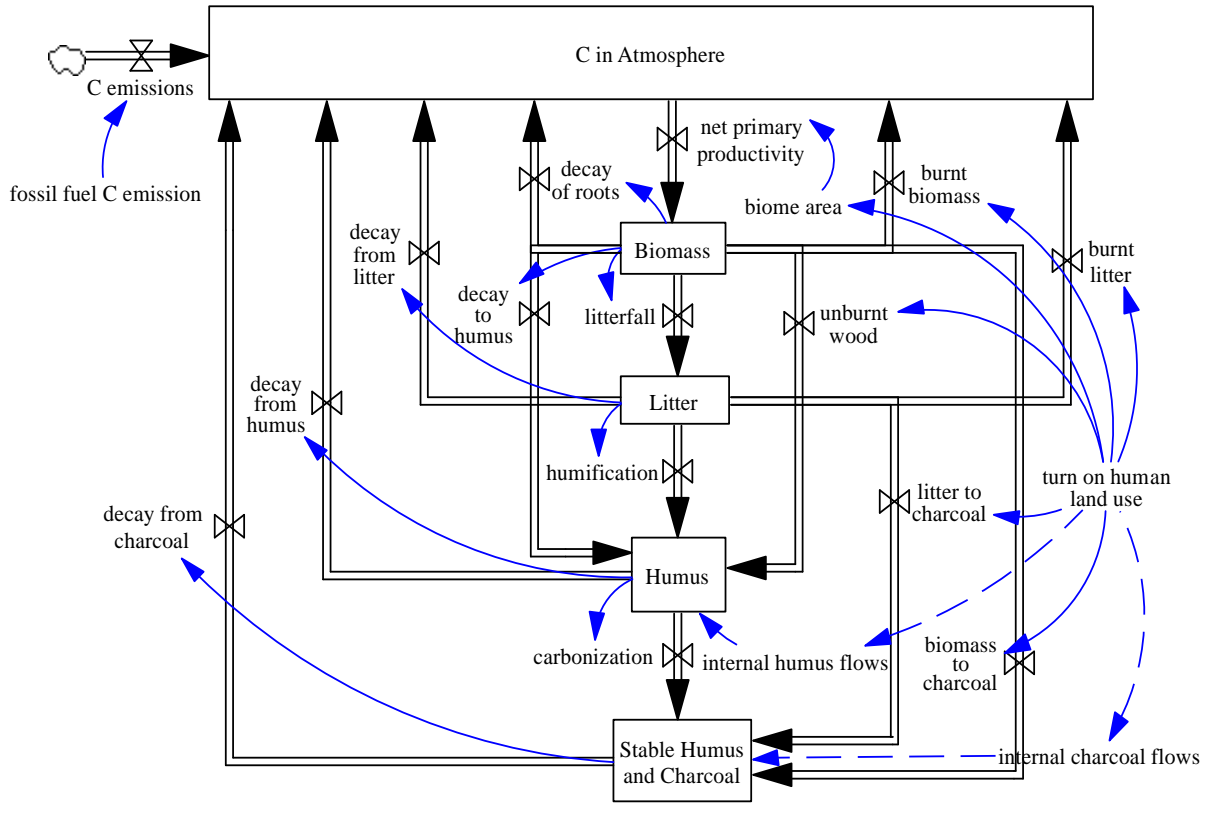


Figure A7 Stock and flow of the *Carbon Sector*

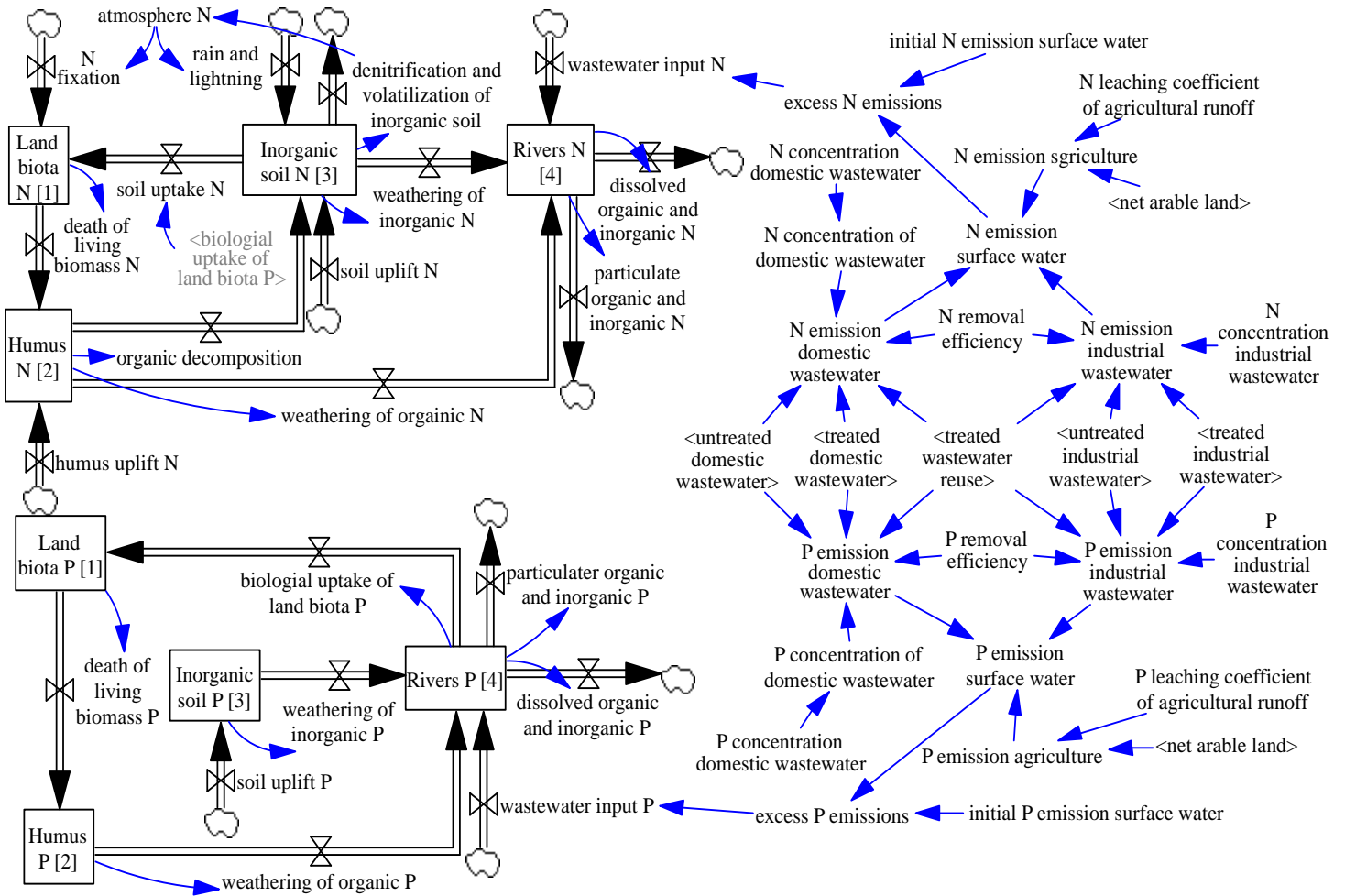


Figure A8 Stock and flow of the *Nutrients Sector*

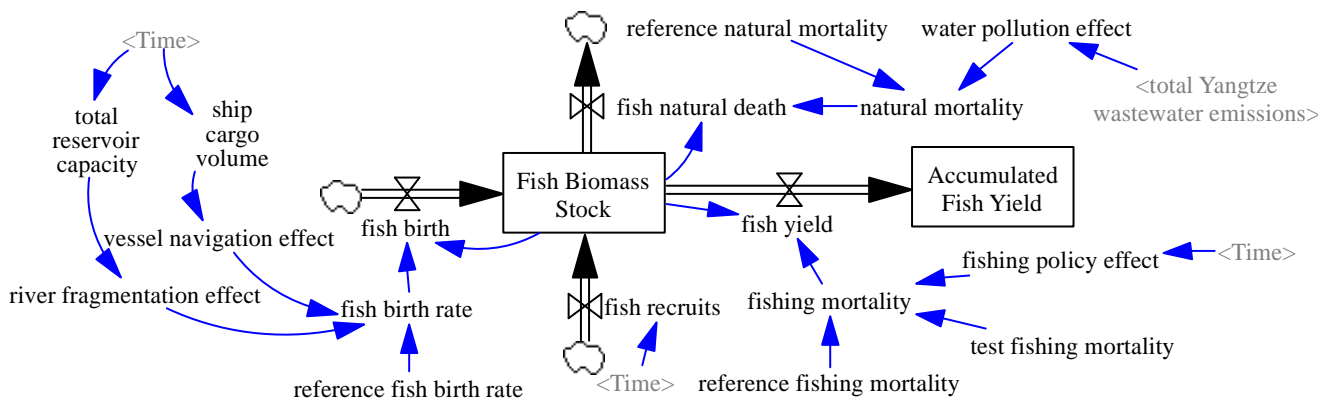



Figure A9 Stock and flow of the *Fish Sector*

## **Appendix B: MODEL AVAILABILITY**

The entire model code is provided in the "ANEMI" GitHub repository located at [https://github.com/FIDS-UWO/anemi\\_yangtze](https://github.com/FIDS-UWO/anemi_yangtze) as a Vensim model file entitled "ANEMI\_Yangtze.mdl". This file can be opened using the Vensim software to view the model structure. A free Vensim PLE licence can be obtained from <https://vensim.com>, which can be used to view the stock and flow diagram that makes up the model structure. Due to the advanced features used in the ANEMI\_Yangtze model, a Vensim DSS license is required to run the model. In addition, as the model was developed using the Vensim DSS for Macintosh Version 5.10d, so it is suggested that a Vensim DSS for Macintosh is used for better display of the model structure.

The ANEMI\_Yangtze.mdl is already set for the base run. No more data or action is needed. All the user has to do is open the model, click on the  button to run the model and obtain the base run simulation results.

The base run simulation results are provided in Appendix C.



## Appendix C: BASE RUN MODEL RESULTS

To test the capabilities of ANEMI\_Yangtze, this section focuses on the application of the model system to the baseline policy scenario. Under the baseline, all the policies shall remain the 2015 values during the simulation. Specifically, the one-child policy shall remain unchanged for the *Population Sector*, the intensity of water withdrawals/consumptions in industry and agriculture for the *Water Sector*, the *energy shares* among different energy sources for the *Energy Sector*, and the *fishing mortality* for the *Fish Sector* shall all remain their 2015 values respectively. The N/P removal efficiency in the *Nutrient Sector* shall be 0. The exogenous inputs of precipitation and temperature shall use their historical average annual data.

Simulation results from 1990 to 2015 were compared to historical data as seen in **Figures A10-15**.

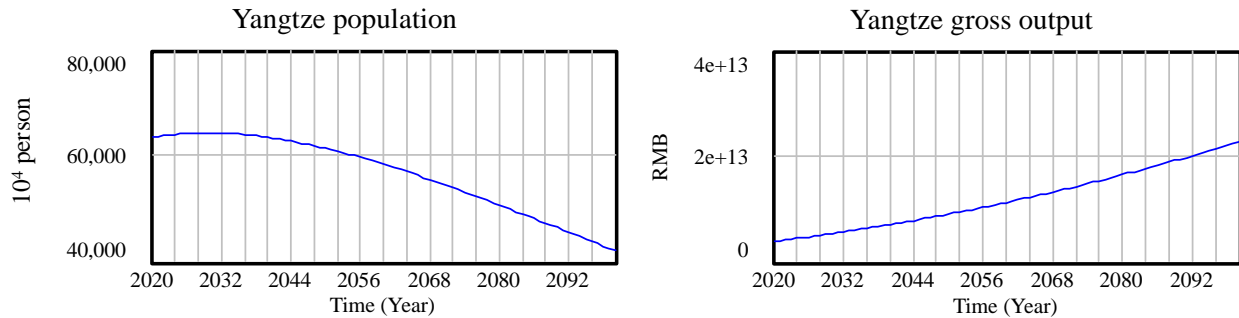


Figure A10 Social-economic behaviours of the Yangtze Economic Belt

The dynamic system behaviours of population and economic output are shown in **Figure A10**. As can be seen, the *population* in Yangtze Economic Belt Economic peaks around 2030 and then decreases to around 400 million by 2100 when only one child is allowed for each family. Yangtze Economic Belt's *gross output* rises gradually up to 22 trillion 1990 RMB by the end of the simulation.

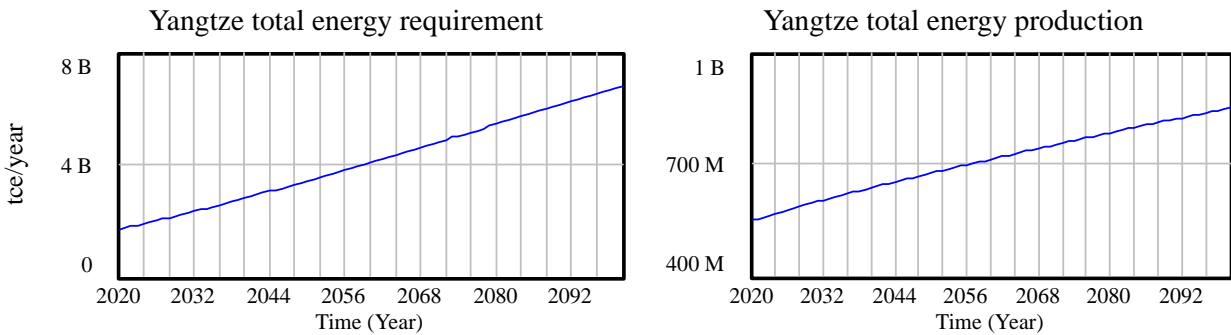


Figure A11 *Energy Sector* system behaviours of the Yangtze Economic Belt

The dynamic system behaviours of energy are shown in **Figure A11**. As can be seen, *energy requirement* shares a similar behaviour mode of *gross output* as its calculation is based on every unit economic output and reaches about 6.7 billion tce by 2100. *Energy production*, however, grows very slowly when compared to *energy requirements*. This is partly due to the general low reserve of fossil fuel in the Yangtze Economic Belt region, so energy production is negatively affected by the remaining resource factor. Another factor that contributes to the slow growth of energy production is the relatively low share of renewable resources (about 15%) even though Yangtze River Basin has abundant hydro resources as the energy shares among different energy sources remain their 2015 values during the whole simulation.

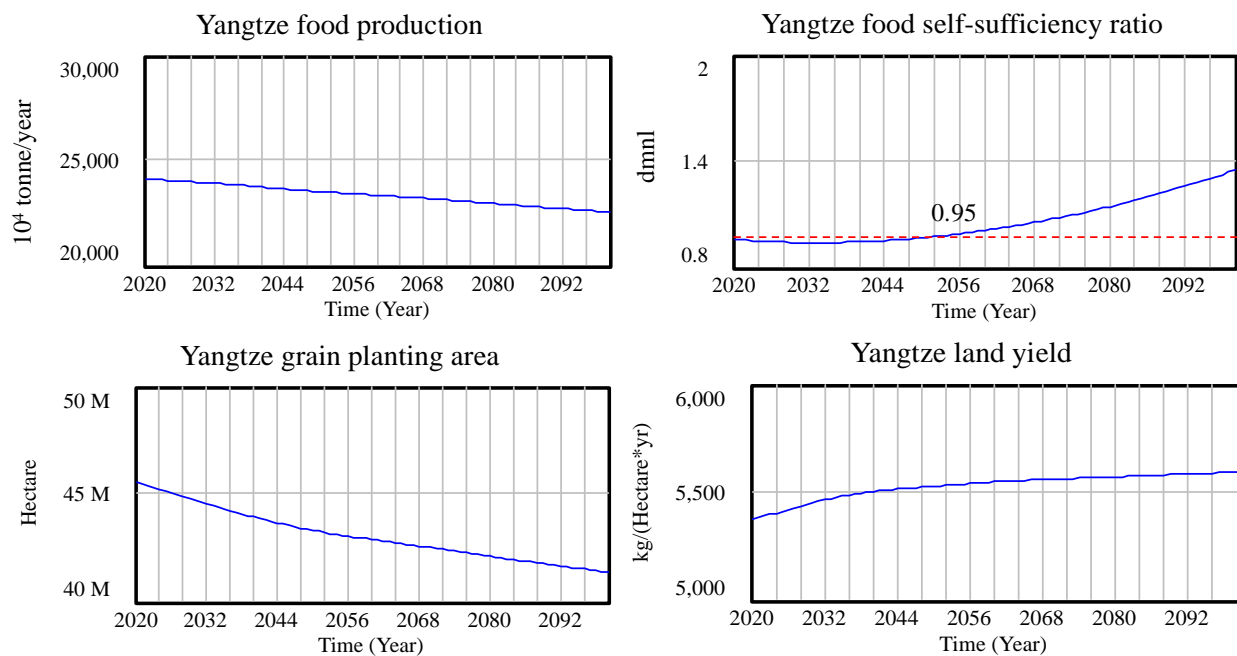


Figure A12 System behaviours in the food sector of the Yangtze Economic Belt

The dynamic system behaviours of food are shown in **Figure A12**. As can be seen, the dynamic behaviour of *food production*, which is determined by both the *land yield* and the *grain planting area*, exhibits a declining behaviour, indicating that the effects of an increase in *land yield* are outpaced by the decrease in the *grain planting area*. The decline in the *grain planting area* is caused by a reduction in *agricultural land*. The *food self-sufficiency ratio* increases to its desired value of 0.95 around 2050. After 2050, the increase continues because of the drastic decrease of population size (shown in **Figure A10**).

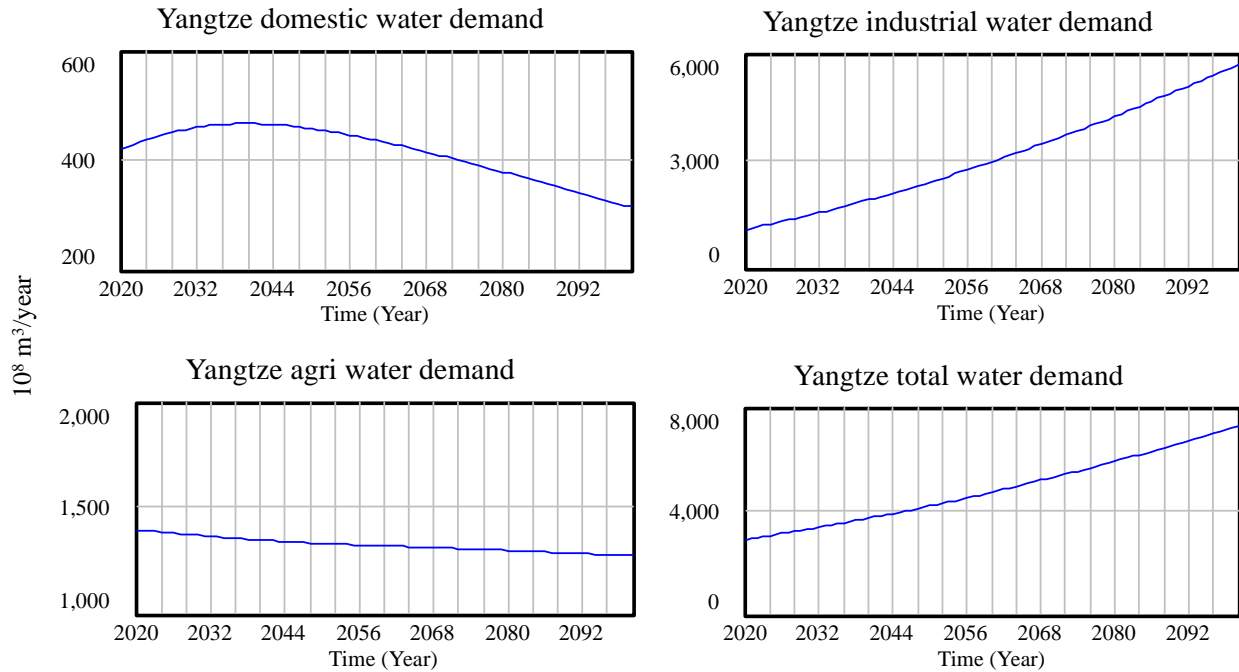


Figure A13 System behaviours of water demand in the Yangtze Economic Belt

The dynamic system behaviours of *water demand* are shown in **Figure A13**. As can be seen, *domestic water demand* follows a pathway that is almost identical to that of the *population* (**Figure A10**), except that the peak of *domestic water demand* comes around 2040, which is 10 years later than the *population* peak. This is due to the *domestic structural water intensity* increases at first with the rise in *GDP per capita* and then stabilizes around 2040. *Industrial water demand* exhibits a strong rise trend because of the considerable increase of *energy consumption*, which equals the *energy requirement* value as shown in **Figure A11**. *Agricultural water demand*, however, shows a decline mode during the simulation. When comparing *agricultural water demand* to *industrial water demand*, it is found that agriculture is the largest water user sector before 2030, however after 2030 industrial sector far dominates the water use. The total water demand by 2100 approaches  $8,000 \text{ } 10^8 \text{ m}^3/\text{year}$ .

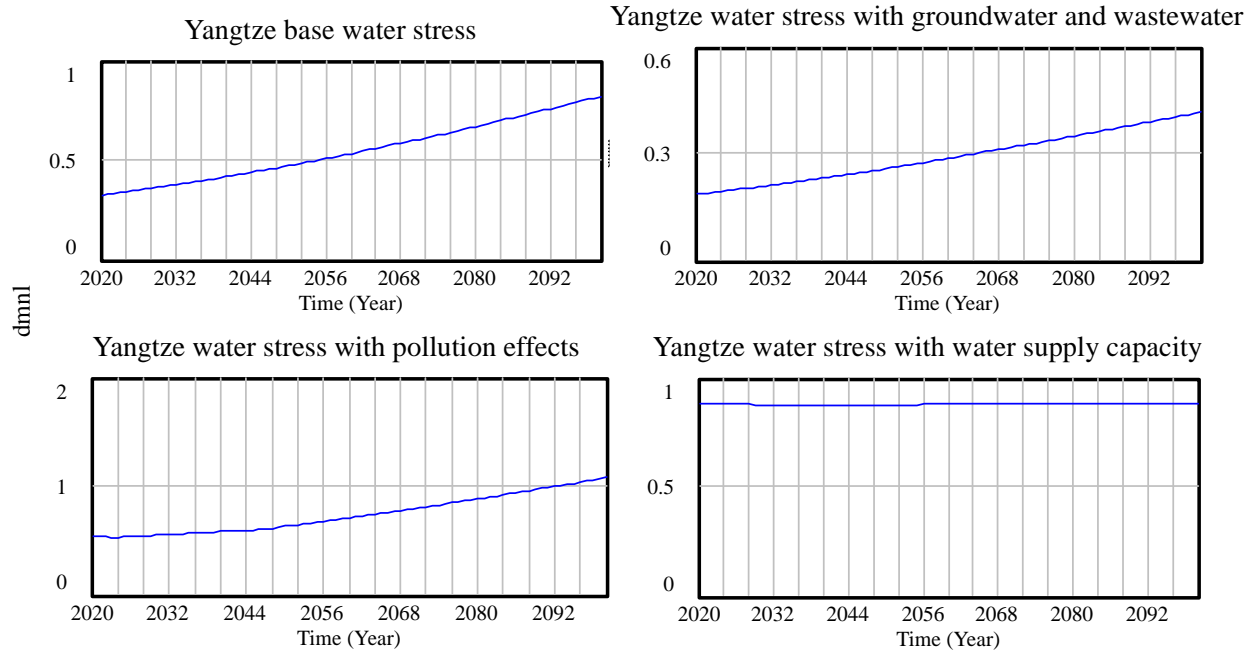


Figure A14 System behaviours of water stress in the Yangtze Economic Belt

**Figure A14** shows the dynamic behaviours of *water stress* under different definitions. Please refer to section 4.6 of the report for detailed definitions of water stress. As shown in Figure A14 the *water stress* falls below the critical value of 1.0 in most cases except when taking water pollution effects into account, indicating that the water resources in the Yangtze Economic Belt are sufficient to support the development of the economic belt.

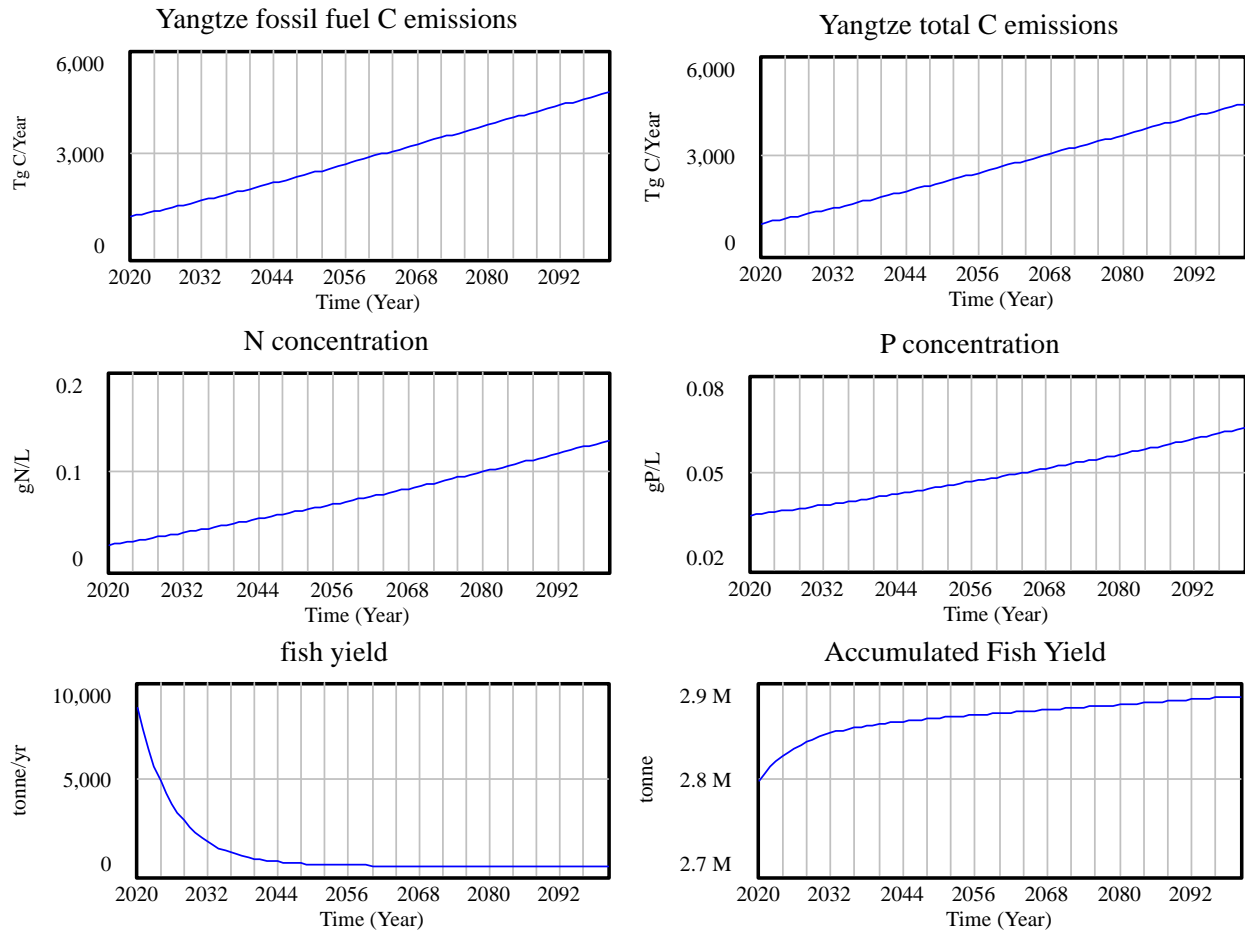


Figure A15 Eco-environmental behaviours of the Yangtze Economic Belt

The eco-environmental system behaviours of the Yangtze Economic are shown in **Figure A15**. As can be seen, the fossil fuel and total carbon emissions and the nitrogen and phosphorus concentrations rise all the way to the end of simulation under the current policy scenario. The Yangtze *fish yield* drops drastically, which confirms that the Yangtze river has come to a stage where there is no fish to catch if there is no fish ban policy.

## **Appendix D: PREVIOUS REPORTS IN THE SERIES**

ISSN: (Print) 1913-3200; (online) 1913-3219

In addition to 78 previous reports (No.01 – No.078) prior to 2012

Samiran Das and Slobodan P. Simonovic (2012). Assessment of Uncertainty in Flood Flows under Climate Change. Water Resources Research Report no. 079, Facility for Intelligent Decision Support, Department of Civil and Environmental Engineering, London, Ontario, Canada, 67 pages. ISBN: (print) 978-0-7714- 2960-6; (online) 978-0-7714-2961-3.

Rubaiya Sarwar, Sarah E. Irwin, Leanna King and Slobodan P. Simonovic (2012). Assessment of Climatic Vulnerability in the Upper Thames River basin: Downscaling with SDSM. Water Resources Research Report no. 080, Facility for Intelligent Decision Support, Department of Civil and Environmental Engineering, London, Ontario, Canada, 65 pages. ISBN: (print) 978-0-7714-2962-0; (online) 978-0-7714- 2963-7.

Sarah E. Irwin, Rubaiya Sarwar, Leanna King and Slobodan P. Simonovic (2012). Assessment of Climatic Vulnerability in the Upper Thames River basin: Downscaling with LARS-WG. Water Resources Research Report no. 081, Facility for Intelligent Decision Support, Department of Civil and Environmental Engineering, London, Ontario, Canada, 80 pages. ISBN: (print) 978-0-7714-2964-4; (online) 978-0-7714- 2965-1.

Samiran Das and Slobodan P. Simonovic (2012). Guidelines for Flood Frequency Estimation under Climate Change. Water Resources Research Report no. 082, Facility for Intelligent Decision Support, Department of Civil and Environmental Engineering, London, Ontario, Canada, 44 pages. ISBN: (print) 978-0-7714- 2973-6; (online) 978-0-7714-2974-3.

Angela Peck and Slobodan P. Simonovic (2013). Coastal Cities at Risk (CcaR): Generic System Dynamics Simulation Models for Use with City Resilience Simulator. Water Resources Research Report no. 083, Facility for Intelligent Decision Support, Department of Civil and Environmental Engineering, London, Ontario, Canada, 55 pages. ISBN: (print) 978-0-7714-3024-4; (online) 978-0-7714-3025-1.

Roshan Srivastav and Slobodan P. Simonovic (2014). Generic Framework for Computation of Spatial Dynamic Resilience. Water Resources Research Report no. 085, Facility for Intelligent Decision Support, Department of Civil and Environmental Engineering, London, Ontario, Canada, 81 pages. ISBN: (print) 978-0-7714-3067-1; (online) 978-0-7714-3068-8.

Angela Peck and Slobodan P. Simonovic (2014). Coupling System Dynamics with Geographic Information Systems: CCaR Project Report. Water Resources Research Report no. 086, Facility 56 for Intelligent Decision Support, Department of Civil and Environmental Engineering, London, Ontario, Canada, 60 pages. ISBN: (print) 978-0-7714-3069-5; (online) 978-0-7714-3070-1.

Sarah Irwin, Roshan Srivastav and Slobodan P. Simonovic (2014). Instruction for Watershed Delineation in an ArcGIS Environment for Regionalization Studies. Water Resources Research Report no. 087, Facility for Intelligent Decision Support, Department of Civil and Environmental Engineering, London, Ontario, Canada, 45 pages. ISBN: (print) 978-0-7714-3071-8; (online) 978-0-7714-3072-5.

Andre Schardong, Roshan K. Srivastav and Slobodan P. Simonovic (2014). Computerized Tool for the Development of Intensity-Duration-Frequency Curves under a Changing Climate: Users Manual v.1. Water Resources Research Report no. 088, Facility for Intelligent Decision Support, Department of Civil and Environmental Engineering, London, Ontario, Canada, 68 pages. ISBN: (print) 978-0-7714-3085-5; (online) 978-0-7714-3086-2.

Roshan K. Srivastav, Andre Schardong and Slobodan P. Simonovic (2014). Computerized Tool for the Development of Intensity-Duration-Frequency Curves under a Changing Climate: Technical Manual v.1. Water Resources Research Report no. 089, Facility for Intelligent Decision Support, Department of Civil 57 and Environmental Engineering, London, Ontario, Canada, 62 pages. ISBN: (print) 978-0-7714-3087-9; (online) 978-0-7714-3088-6.

Roshan K. Srivastav and Slobodan P. Simonovic (2014). Simulation of Dynamic Resilience: A Railway Case Study. Water Resources Research Report no. 090, Facility for Intelligent Decision Support, Department of Civil and Environmental Engineering, London, Ontario, Canada, 91 pages. ISBN: (print) 978-0-7714-3089-3; (online) 978-0-7714-3090-9.

Nick Agam and Slobodan P. Simonovic (2015). Development of Inundation Maps for the Vancouver Coastline Incorporating the Effects of Sea Level Rise and Extreme Events. Water Resources Research Report no. 091, Facility for Intelligent Decision Support, Department of Civil and Environmental Engineering, London, Ontario, Canada, 107 pages. ISBN: (print) 978-0-7714-3092-3; (online) 978-0-7714-3094-7.

Sarah Irwin, Roshan K. Srivastav and Slobodan P. Simonovic (2015). Instructions for Operating the Proposed Regionalization Tool "Cluster-FCM" Using Fuzzy C-Means Clustering and LMoment Statistics. Water Resources Research Report no. 092, Facility for Intelligent Decision Support, Department of Civil and Environmental Engineering, London, Ontario, Canada, 54 pages. ISBN: (print) 978-0-7714-3101-2; (online) 978-0-7714-3102-9.

Bogdan Pavlovic and Slobodan P. Simonovic (2016). Automated Control Flaw Generation Procedure: Cheakamus Dam Case Study. Water Resources Research Report no. 093, Facility for Intelligent Decision Support, Department of Civil and Environmental Engineering, London, Ontario, Canada, 78 pages. ISBN: (print) 978-0-7714-3113-5; (online) 978-0-7714-3114-2.

Sarah Irwin, Slobodan P. Simonovic and Niru Nirupama (2016). Introduction to ResilSIM: A Decision Support Tool for Estimating Disaster Resilience to Hydro-Meteorological Events. Water Resources Research Report no. 094, Facility for Intelligent Decision Support, Department of Civil and Environmental Engineering, London, Ontario, Canada, 66 pages. ISBN: (print) 978-0-7714-3115-9; (online) 978-0-7714-3116-6.

Tommy Kokas, Slobodan P. Simonovic (2016). Flood Risk Management in Canadian Urban Environments: A Comprehensive Framework for Water Resources Modeling and Decision-Making. Water Resources Research Report no. 095. Facility for Intelligent Decision Support, Department of Civil and Environmental Engineering, London, Ontario, Canada, 66 pages. ISBN: (print) 978-0-7714-3117-3; (online) 978-0-7714-3118-0.

Jingjing Kong and Slobodan P. Simonovic (2016). Interdependent Infrastructure Network Resilience Model with Joint Restoration Strategy. Water Resources Research Report no. 096, Facility for Intelligent Decision Support, Department of Civil and Environmental Engineering,



London, Ontario, Canada, 83 pages. ISBN: (print) 978-0-7714-3132-6; (online) 978-0-7714-3133-3.

Sohom Mandal, Patrick A. Breach and Slobodan P. Simonovic (2017). Tools for Downscaling Climate Variables: A Technical Manual. Water Resources Research Report no. 097, Facility for Intelligent Decision Support, Department of Civil and Environmental Engineering, London, Ontario, Canada, 95 pages. ISBN: (print) 978-0-7714-3135-7; (online) 978-0-7714-3136-4.

R Arunkumar and Slobodan P. Simonovic (2017). General Methodology for Developing a CFD Model for Studying Spillway Hydraulics using ANSYS Fluent. Water Resources Research Report no. 098, Facility for Intelligent Decision Support, Department of Civil and Environmental Engineering, London, Ontario, Canada, 39 pages. ISBN: (print) 978-0-7714-3148-7; (online) 978-0-7714-3149-4.

Andre Schardong, Slobodan P. Simonovic and Dan Sandink (2017). Computerized Tool for the Development of Intensity-Duration-Frequency Curves Under a Changing Climate: Technical Manual v.2.1. 58 Water Resources Research Report no. 099, Facility for Intelligent Decision Support, Department of Civil and Environmental Engineering, London, Ontario, Canada, 52 pages. ISBN: (print) 978-0-7714-3150-0; (online) 978-0-7714-3151-7.

Andre Schardong, Slobodan P. Simonovic and Dan Sandink (2017). Computerized Tool for the Development of Intensity-Duration-Frequency Curves Under a Changing Climate: User's Manual v.2.1. Water Resources Research Report no. 100, Facility for Intelligent Decision Support, Department of Civil and Environmental Engineering, London, Ontario, Canada, 52 pages. ISBN: (print) 978-0-7714-3152-4; (online) 978-0-7714-3153-1.

Ayushi Gaur, Abhishek Gaur and Slobodan P. Simonovic (2017). Modelling of High Resolution Flow from GCM Simulated Runoff using a Mesoscale Hydrodynamic Model: CAMA-FLOOD. Water Resources Research Report no. 101, Facility for Intelligent Decision Support, Department of Civil and Environmental Engineering, London, Ontario, Canada, 44 pages. ISBN: (print) 978-0-7714-3154-8; (online) 978-0-7714-3155-5.

Jingjing Kong and Slobodan P. Simonovic (2017). Multi-hazard resilience model of an interdependent infrastructure system. Water Resources Research Report no. 102, Facility for

Intelligent Decision Support. Department of Civil and Environmental Engineering, London, Ontario, Canada, 99 pages. ISBN: (print) 978-0-7714-3158-6; (online) 978-0-7714-3159-3.

Andre Schardong, Slobodan P. Simonovic and Dan Sandink (2018). Computerized Tool for the Development of Intensity-Duration-Frequency Curves Under a Changing Climate: Technical Manual v.3. Water Resources Research Report no. 103, Facility for Intelligent Decision Support, Department of Civil and Environmental Engineering, London, Ontario, Canada, 67 pages. ISBN: 978-0-7714-3107-4.

Andre Schardong, Slobodan P. Simonovic and Dan Sandink (2018). Computerized Tool for the Development of Intensity-Duration-Frequency Curves Under a Changing Climate: User's Manual v.3. Water Resources Research Report no. 104, Facility for Intelligent Decision Support, Department of Civil and Environmental Engineering, London, Ontario, Canada, 80 pages. ISBN: 978-0-7714-3108-1.

Schardong, A., S. P. Simonovic and H. Tong (2018). Use of Quantitative Resilience in Managing Urban Infrastructure Response to Natural Hazards: A Web-Based Decision Support Tool - ResilSIMt. Water Resources Research Report no. 105, Facility for Intelligent Decision Support, Department of Civil and Environmental Engineering, London, Ontario, Canada, 112 pages. ISBN: 978-0-7714-3115-7.

Feitoza Silva D. and S. P. Simonovic (2020). Development of Non-Stationary Rainfall Intensity Duration Frequency Curves for Future Climate Conditions. Water Resources Research Report no. 106, Facility for Intelligent Decision Support, Department of Civil and Environmental Engineering, London, Ontario, Canada, 48 pages. ISBN: (print) 978-0-7714-3137-1; (online) 978-0-7714-3138-8.

Braden, J. and S.P. Simonovic (2020). A Review of Flood Hazard Mapping Practices across Canada. Water Resources Research Report no. 107, Facility for Intelligent Decision Support, Department of Civil and Environmental Engineering, London, Ontario, Canada, 64 pages. ISBN: (print) 978-0-7714-3143-2; (online) 978-0-7714-3144-9.

Patrick A. Breach and Slobodan P. Simonovic (2020). ANEMI 3: Tool for investigating impacts of global change. Water Resources Research Report no. 108, Facility for Intelligent Decision

Support, Department of Civil and Environmental Engineering, London, Ontario, Canada, 134 pages. ISBN: (print) 978-0-7714-3145-6; (online) 978-0-7714-3146-3.

Mohit P. Mohanty and Slobodan P. Simonovic (2020). A comprehensive framework for regional floodplain mapping. Water Resources Research Report no. 109, Facility for Intelligent Decision Support, Department of Civil and Environmental Engineering, London, Ontario, Canada, 58 pages. ISBN: : (print) 978-0-7714-3147-0 ; (online) 978-0-7714-3148-7.

Bogdana Sredojevic, Mohit P. Mohanty and Slobodan P. Simonovic (2020). Regional Analysis of Population Exposure to Flooding in Canada. Water Resources Research Report no. 110, Facility for Intelligent Decision Support, Department of Civil and Environmental Engineering, London, Ontario, Canada, 61 pages. ISBN: (print) 978-0-7714-3151-7 ; (online) 978-0-7714-3152-4.